BASIN EFFECTS ON SURFACE WAVE AMPLIFICATION

A DISSERTATION

Submitted in partial fulfillment of the requirements for the award of the degree

of

MASTER OF TECHNOLOGY

in

EARTHQUAKE ENGINEERING

(With Specialization in Seismic Vulnerability and Risk Assessment)

By

SHEETAL ASWAL

(14553009)

Under the Guidance of

Dr. J.P. NARAYAN

DEPARTMENT OF EARTHQUAKE ENGINEERING

INDIAN INSTITUTE OF TECHNOLOGY ROORKEE

ROORKEE – 247667

MAY 2016

CANDIDATE'S DECLARATION

I hereby declare that the thesis work, which is being presented in this dissertation entitled, "**Basin Effects on Surface Wave Amplification",** in the partial fulfillment of the requirements for the award of the degree of **Master of Technology** in **Earthquake Engineering**, with specialization in **Seismic Vulnerability & Risk Assessment**, submitted in the Department of Earthquake Engineering, Indian Institute of Technology Roorkee, is an authentic record of my own work carried out for a period from June 2015 to May 2016 under the guidance of **Dr. J.P. NARAYAN**, Professor, Department of Earthquake Engineering, Institute of Technology Roorkee, Roorkee.

The matter embodied in this report has not been submitted by me for the award of any other degree or diploma of this Institute or any other University/Institute**.**

SHEETAL ASWAL
(14553009)
M.Tech
SVRA

Place: Roorkee
Date: MAY, 2016

CERTIFICATE

This is to certify that the above statement made by the candidate is correct to the best of my knowledge.

Dr. J.P.Narayan
Professor
Department of Earthquake Engineering
Institute of Technology Roorkee

Place: Roorkee
Date: MAY, 2016

ACKNOWLEDGEMENT

The success of this thesis depends largely on my guide Dr. J.P. Narayan, Professor, Department of Earthquake Engineering, I.I.T. Roorkee. I have been really fortunate to have him as my guide and mentor and would like to show my greatest gratitude to him for his tremendous support and help. Without his encouragement and guidance this dissertation would not have materialized.

The encouragement and guidance of many others has also been a great help and motivation all throughout the completion. I take this opportunity to express my gratitude to my family, my dear friends and all the people who have been instrumental in the successful completion of this seminar.

SHEETAL ASWAL

(14553009)

M.Tech (SVRA)

Department of Earthquake Engineering

I.I.T Roorkee

Place: Roorkee

Date: 2 MAY 2016

ABSTRACT

For the simulation of Rayleigh wave, fourth order staggered grid wave FD program was used for both the homogeneous and basin models (Narayan and Kumar, 2014). The Gabor wavelet was used for the source excitation. The effects of basin shape ratio, impedance contrast and the shape of basin on the Rayleigh wave is analyzed. The simulation of this wave revealed the mode transformation and amplification of the Rayleigh wave at the basin-edge. The spectral amplification increased when the depth was increased at the left edge of the basin as well as in the entire basin. In case of higher frequencies the spectral amplification decreased with the increase of basin depth. The spectral amplification was found to be highest in case of triangular basin. Similarity between the elliptical model and gentle slope trapezoidal model was obtained. The increase in average spectral amplification was found to be increasing with increase in IC. The decrease in spectral amplitude while moving away from the basin edge was found due to the damping effects in the basin.

CONTENTS

LIST OF FIGURES

LIST OF TABLES

CHAPTER #1

INTRODUCTION

1.1. GENERAL

When the focal depth of an earthquake is shallow high frequency Rayleigh waves are generated. These high frequency Rayleigh waves when enters the basin, reflects and transmits their energy accordingly. Such waves are called 'basin-transduced surface' wave or the BTR wave. When these Rayleigh waves enter into the basin complex mode transformation takes place ,as one single mode of these wave gets converted to different modes from rock to the basin i.e., mode conversion between two different media, takes place. Structural damage in basin is significantly high when compared to its surrounding rocks or the basins from place to place. There are many parameters which results in the body wave amplification namely damping, focusing effects, impedance, resonance, basin edge effects.

The Surface waves can be very damaging in case of basin and other topographical effects but the study on complex behavior of BTR-waves at edge of basin is very limited. The long span structures are specially effected in such case when the BTR waves have high amplitude and variability in ground motion caused .Large strain in long-span structures) can occur due to these high frequency Rayleigh waves in case of a shallow earthquake, if the span of the structures matches with the wavelength of Rayleigh waves.

1.2. OBJECTIVE AND SCOPE OF THESIS:

A lot of research has been carried out to analyze the effects of body waves on the structures but a very limited work has been done to analyze the effects of surface waves amplification in the basin. There are various factors due to which the study is so limited, like the non availability of earthquake records containing surface waves across the basin, no efficient methodology etc.

The aim of this dissertation work is to find the effects of basin on the surface waves. To fulfill this objective we need to first generate the Rayleigh wave in the rock and correspondingly let it propagate in the basin. Thereafter we can compare the computed response of surface waves in the rocks to the computed response of the basin at different distance from the centre of basin to find out the amount of spectral amplification theoretically.

In chapter 2, various factors effecting the surface waves in basin are described in brief. The finite difference method, and the methodology has also been explained in brief in this chapter. Simulation of Rayleigh wave in homogeneous viscoelastic medium using Gabor wavelet and its variation due to different source depth has been documented in the chapter 3. In chapters 4 and 5, details of simulation of BTR wave with effects of varying impedance contrast, depth of basin, and shape of basin has been calculated theoretically.

1.3 FUTURE RESEARCH WORK

The work can further be carried out to simulate the basin transduced Rayleigh waves in a 3D basin. The work can further be extended in case of multi layered 2D or 3D basins.

CHAPTER #2

EFFECT OF VARIOUS FACTORS ON BTR WAVE CHARACTERISTICS AND FINITE DIFFERENCE METHOD

2.1 INTRODUCTION:

A basin is made of geologically younger alluvial deposits and sedimentary rocks in which there is comparatively lower seismic velocity than the surrounding rocks or the underlying rock on which they are supported. The basin's shape, size, geometry, depth contribute in different ways to the damage of structures during earthquake. The amplitude of Rayleigh waves can further be amplified many times in basin than in rocks due to the various rheological parameters. The amplitude of shaking in basin can be 12 times stronger than the surrounding rocks. The effect of local geology should also be counted in the studies of seismic risk assessment and seismic microzonation and seismic design of structures.

2.2 BASIN –EFFECTS ON GROUND MOTION CHARACTERISTICS:

2.2.1 Impedance contrast:

The meaning of impedance is opposing the particle motion of seismic wave propagation. Impedance contrast arises at the boundary of two mediums having different impedance, when wave travels through them. Impedance is simply the multiplication of the density of the medium and the velocity of seismic wave in either case of rock or soil. When the seismic waves propagate from the rock their velocity is high, but as they enter into the lower density basin they become slow. Due to the lowering of velocity in the basin the amplitude of the waves increase suddenly in accordance to the law of conservation of energy due to which they get bigger in amplitude to carry the same amount of energy. Neglecting the effects of soil damping and the scattering, the conservation of elastic wave energy requires that the flow of energy (energy flux $\rho V_s u^2$) from depth to ground surface be constant. Hence due to the decrease in the density and the velocity of the medium as

wave approaches the ground surface, the particle velocity must increase. This can lead to substantial amount of damage in the softer soil deposits

2.2.2 Resonance:

When a seismic wave enters into a basin multiple reflections occurs from top to the bottom of the soil deposit due to the bounded medium. This causes a standing wave in the medium. During the back and forth motion some energy goes in the rock and finally the amplitude becomes zero due to damping. The fundamental frequency (resonance frequency) for a single horizontal soil layer can be computed as follows:

$F_0 = V_s / 4H$ (Fundamental mode) and $F_N = (2N + 1) F_0$ (Harmonics)

Where $\overline{V_s}$ is the shear wave velocity in the soil layer and 'H' is the thickness of soil layer.
The spectral amplification factor are related to the sediment and the underlying bedrock and to the damping. The maximum spectral amplification at the fundamental frequency is equal to

$$A_0 = \frac{1}{\left(\frac{1}{IC} + 0.5\pi\varepsilon_1\right)}$$

Where ε_1=(1/2Q) is the damping in sediment, $IC = \frac{\rho_2 V_{s2}}{\rho_1 V_{s1}}$ (Ratio of impedance of rock to impedance of overlying soil deposit).
When the signal frequency matches with the fundamental frequency of the soil layer or with the higher harmonics there is a tremendous increase in the spectral ground motion amplification. So the natural frequency of structures should be kept below F_0 to avoid double resonance.

2.2.3 Damping:

The soil medium is imperfectly elastic due to which when the medium particles interact with their neighbor particles absorption of energy takes place. After each cycle a part of energy is lost instead of getting transferred through the medium. This decrease or the attenuation of the seismic waves is called the anelastic damping. This anelastic damping is described by a parameter known as quality factor (Q). It is the fractional loss of energy in each cycle.

$$\frac{2\pi}{Q} = -\frac{\Delta E}{E}$$

Where ΔE is energy lost per cycle and E is the total energy saved in the wave.

2.3 METHODOLOGY

2.3.1 FINITE DIFFERENCE METHOD

There are various numerical methods to simulate the Rayleigh waves but the complex medium requires a simplest method. Hence we use the finite difference method which is simple and easy to handle and implement in the computer programs. We use the explicit time domain finite difference method of simulation because in this method. We can compute the snapshots of the seismic wave field. With the help of snapshots we can clearly see the seismic behaviour of seismic waves in a complex medium. The wave entering and its behaviour in the basin can also be seen.

There are different parameters used while implementing the finite difference method like absorbing boundary condition at the model edges, anelastic damping parameters. When the Rayleigh waves propagate they are reflected back at the edges of the basin , to show this attenuation of amplitude of the edge reflected waves we need absorbing boundary condition. In the past various absorbing boundary condition have been developed and implemented along the model edges (Clayton and Engquist, 1977; Israeli and Orszag, 1981).

We need stability conditions in order to make the scheme stable for the various homogenous and heterogeneous models. To avoid numerical stability problems, the stability condition proposed for various schemes should be followed. Narayan and Kumar (2010) concluded that the staggered grid P-SV scheme with fourth order accuracy is stable for both the homogenous and heterogeneous models, if the following stability condition is locally satisfied.

Condition for P-wave, SH- wave and P-SV wave FD simulation with second order special accuracy:

$$\frac{\mathrm{Vp}\Delta\mathrm{t}}{\min\left(\Delta\mathrm{x},\Delta\mathrm{z}\right)} \leq 0.71$$

Condition for P-wave, SH- wave and P-SV wave FD simulation with fourth order special accuracy:

$$\frac{\mathrm{Vp}\Delta\mathrm{t}}{\min\left(\Delta\mathrm{x},\Delta\mathrm{z}\right)} \leq 0.606$$

Where Vp is P-wave velocity, Δx and Δz are the grid size in X and Z-directions at a particular node.

The desired earth model is converted into the finite difference model using the cells. The earth model is subdivided into cells following the stability technique. The size of the cell shall neither be too small nor too large. If it is too small the computational time increases and also the data handling can become difficult. If the cell size is too large the dispersion of the signal can occur and this dispersion will increase with travel time. This phenomenon is called grid dispersion. Due to the grid dispersion the velocity varies with each frequency that means the lower frequency signal will travel faster than the high frequency signal. Minimum 5 to 6 grid points are required for each wavelength in the fourth order spatial accuracy to avoid the grid-dispersion and at least 10 grid spacing should be used to sample the wavelength λ in order to avoid grid dispersion of the phase and group velocities for the wavelength λ in second order spatial accuracy.

2.3.2 FREE SURFACE BOUNDARY CONDITION

The implementation of boundary conditions is important at the free surface for greater accuracy of FD method. There are two types of free surface boundary conditions:

i. Vacuum formulation: In this method all the elastic parameters are kept equal to zero and the density above the free surface is reduced substantially (Boore, 1972). This approach catches our attention as same finite difference equation are implemented in interior of model. It is also good for calculating displacement.

ii. Stress imaging technique: In this method explicit boundary conditions are applied to the stress tensor components located at the grid plane coinciding with the free surface

(Lavander, 1988; Graves, 1996). The stress tensors components are assumed to be anti-symmetry with respect to the free surface. In our FD Method we using vacuum formulation.

2.4 GABOR WAVELET

This wave is important since the results or output from the simulation of Gabor wavelet gives us minimum deviation from the mean value in both Time and Frequency analysis. Therefore the results given by using this wave in simulation are more certain and closer to reality. Due to their importance they are used widely in image processing, face detetection techniques and analyzing neurons in the human visual system. The mathematical relation for generating the Gabor is

$$S(t) = Exp(-\alpha)cos[\omega_P(t - t_S) + \varphi]$$

where $\alpha = \left[\frac{\omega_P(t-t_S)}{\gamma}\right]^2$, fp is predominant frequency, γ controls the oscillatory character, t_S controls the duration (duration=2 t_S) and φ is phase shift. Figure 2.1a&b shows the generated Gabor pulse for fp=4 , γ= .25 , t_S=1.5 and φ=0 . and its spectra.

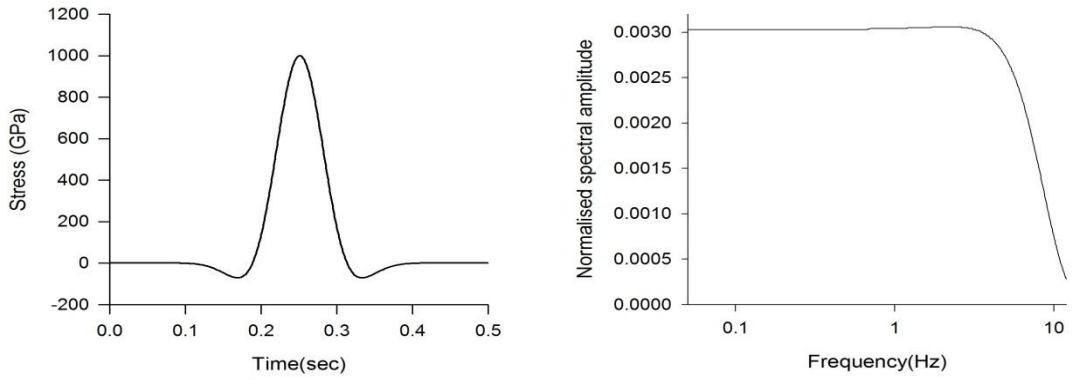

Figure 2.1 Gabor wavelet time domain and frequency domain analysis.

CHAPTER #3

ANALYSIS OF THE HOMOGENEOUS AND BASIN RESPONSES USING GABOR WAVELET AS A SOURCE EXCITATION FUNCTION

3.1. HOMOGENOUS HALF SPACE MODEL

A half space homogeneous model of rock was taken. The P wave and S wave velocity and other parameters such as density, quality factor and Poisson's ratio for the model are given in Table 3.1. Further, The anelastic coefficients and unrelaxed moduli for the rock are given in Table 3.2. The model was discretised with two grid size one large grid 10 m and small grid of 5 m to avoid the computational efforts. The basin is using the 5 grid size. Time step was taken as 0.001 s in all the simulations. Seismic response was computed at 25 stations. The stations were at a distance of 50 m from each other. The first receiver is at a distance of 900 m from the source. The point source was generated at a depth of 100m from the free surface and at a distance of 1100 m from the left boundary of the model. The shallow point source has caused high frequency Rayleigh wave generation. The figure 3.1 shows the cross section of homogenous viscoelastic half space model.

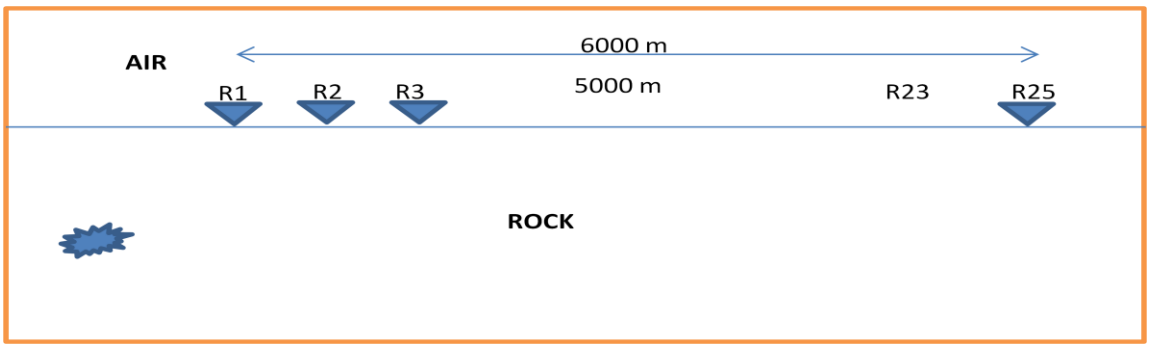

Figure. 3.1 Homogenous viscoelastic half space model.

Table 3.1 The P-wave velocity, S-wave velocity, density, quality factor and Poisson's ratio for considered homogeneous half-space model.

MATERIAL	Vs(m/s)	Vp(m/s)	Density (g/cc)	Poisson ratio	Quality factor(Q)
Rock	1800	3114	2.4	0.25	180

Table 3.2. Unrelaxed moduli and Anelastic coefficients for homogeneous rock.

	Unrelaxed moduli			Anelastic coefficients		
	μ_u (GPa)	**K** (GPa)	λ_u (GPa)	Y_l^{α} (1=1,4)	Y_l^{β} (1=1,4)	Y_l^{λ} (1=1,4)
ROCK	7.8605	23.4185	7.6975	0.005382384	0.009147663	0.009895534
				0.004554900	0.007794690	0.008440975
				0.004580726	0.007871273	0.008530337
				0.005516699	0.0095455956	0.010356537

The horizontal and vertical components of ground motion are shown in the figures 3.2, respectively. The amplitude of the horizontal component is lesser than that in the vertical component since medium is homogeneous. The trace shown in figure 3.3 were normalised with the average of maximum amplitude in the horizontal and vertical components of the traces recorded at the epicentre. The distances shown in the figure 3.3 is with respect to the 13^{th} receiver station which is located at the centre of the receiver array. There is only minor decrease of amplitude of Raleigh wave with the distance travelled due to damping. In case of Rayleigh wave simulation in a 2D plane there is no divergence effect.

Figure 3.3 shows the comparison of spectral amplitudes in the horizontal and vertical components for the homogeneous model at different locations. The Rayleigh wave having frequency 5.5 Hz has the largest spectral amplitude for the considered focal depth, damping and the source spectra. There is only minor decrease of spectral amplitude of Rayleigh waves with the distance travelled due to the viscoelastic damping in the

homogeneous rock. The spectral amplitudes in the vertical components are larger than that in the horizontal components, which is obvious one in case of Rayleigh propagating in the homogeneous medium.

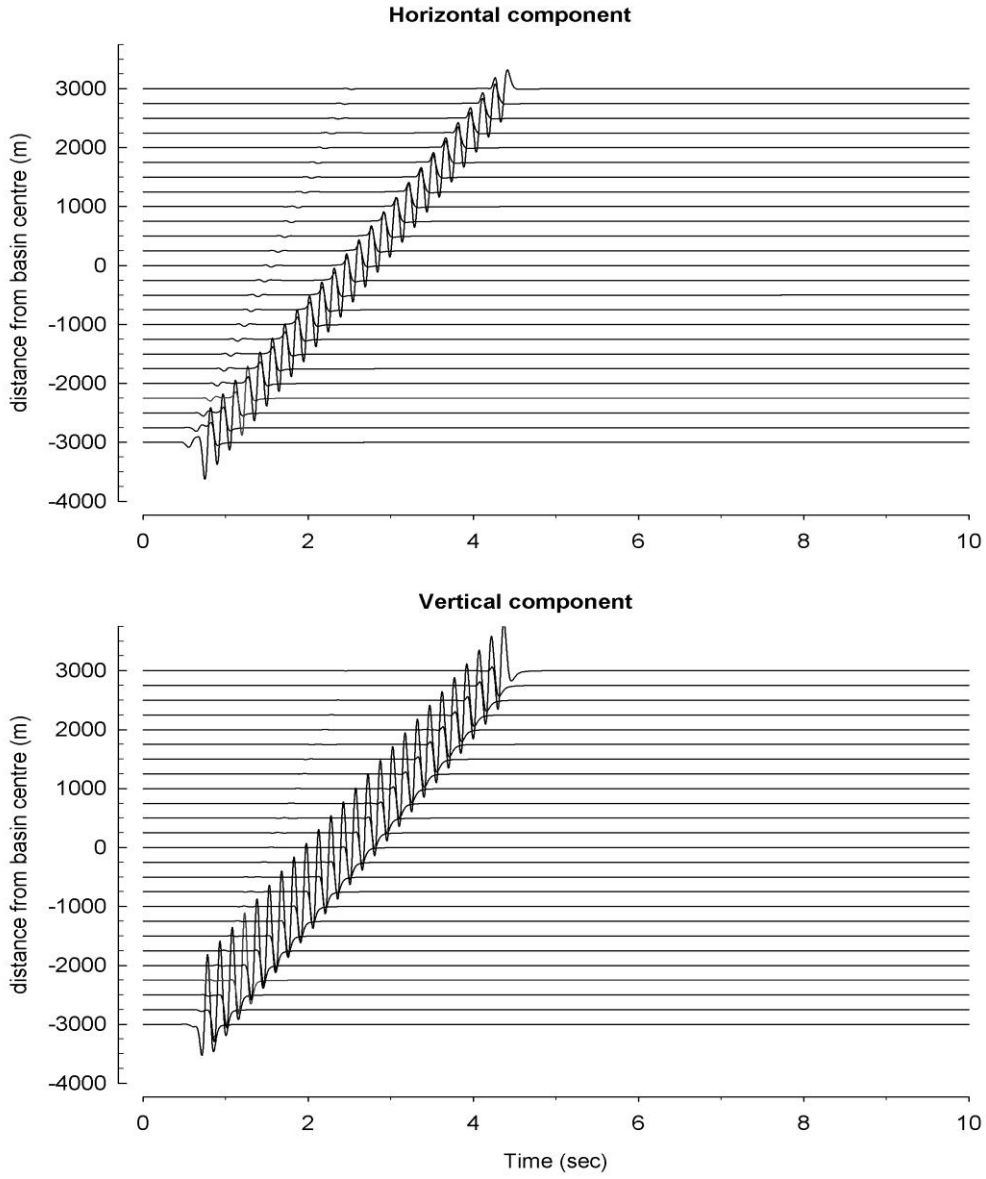

Figure 3.2 Seismic response of homogeneous viscoelastic model on a horizontal array at 25 stations for 100m source depth.

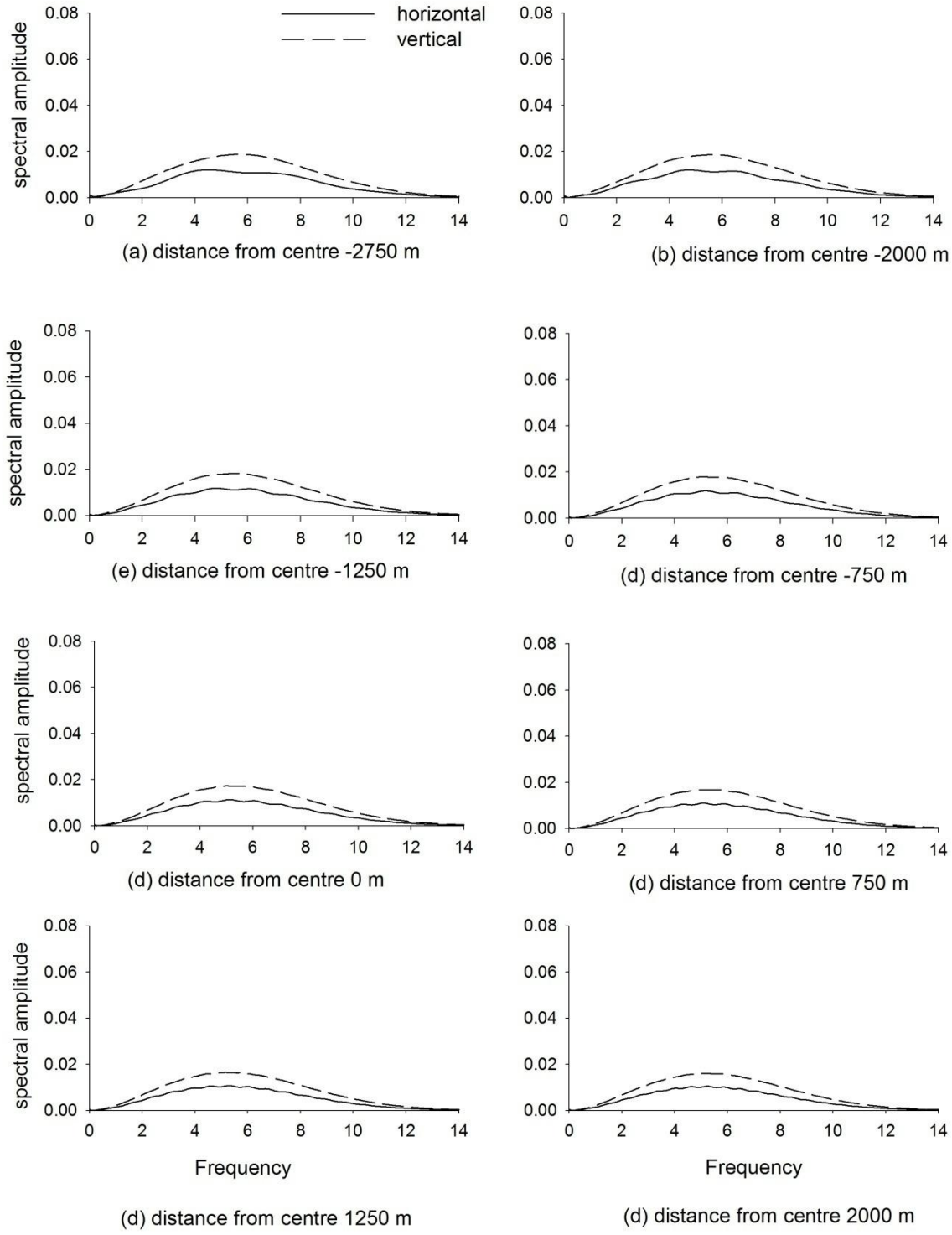

Fig.ure 3.3 Spectral amplitude of both components of Rayleigh waves recorded at different distances from centre of basin for homogeneous model.

3.2. BASIN MODEL

An elliptical basin model has been considered to study the various effects of basin on the characteristics of BTR waves, dispersion and damping effects. The model of the basin is shown in the figure 5. The basin starts at a distance of 1400m from the epicentre of point source and extents at a length of 5000 m. The source is generated at 1100 m from the left edge of the model. The right edge of the model is at a distance of 1100 m from the 25th receiver point. The maximum depth of basin is 600 m. The basin has radius of curvature as 1086 m. The grid size used during the descretisation of basin model is of different dimension in the same entire range, in order to avoid the computational memory and time. The grid size used is 5 and 10.The velocities and the quality factors for the P- and S-waves at reference frequency 1.0 Hz, density, anelastic coefficients and unrelaxed moduli for the sediment are given in table 3. Two receivers are placed before the basin and two receivers at the end of the basin on the rock in order to incorporate the basin edge effects also.

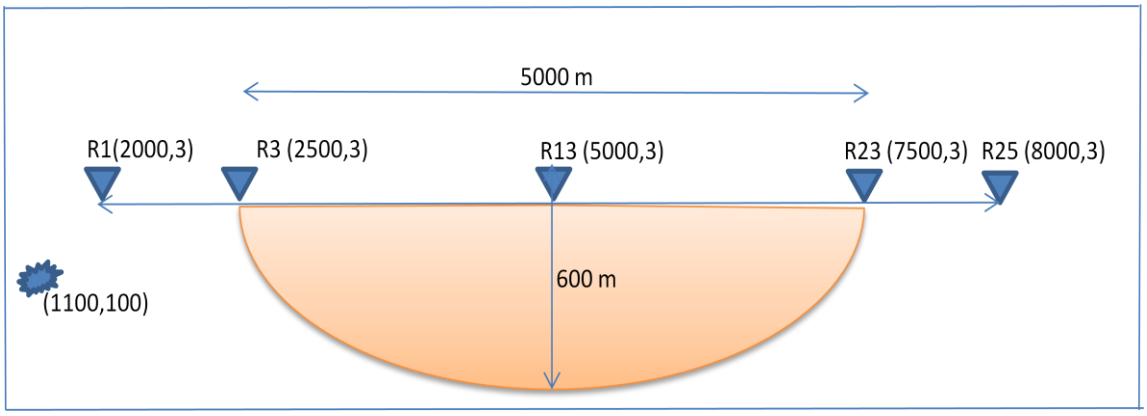

Figure 3.4 Elliptical basin model along with source receiver configuration.

Table 3.3 Basin parameters.

MATERIAL	Vs(m/s)	Vp(m/s)	Density (g/cc)	Poisson ratio	Quality factor (Q)
Soil	500	971	2.0	.25	50

Table 3.4 Unrelaxed moduli and Anelastic coefficients for sediment and rock

	Unrelaxed moduli			Anelastic coefficient		
	μ_u (GPa)	**K**(GPa)	λ_u(GPa)	$Y_l^{\alpha}(1=1,4)$	Y_l^{β} (1=1,4)	$Y_l^{\lambda}(1=1,4)$
Rock	7.8605	23.4185	7.6975	0.005382384	0.009147663	0.009895534
				0.004554900	0.007794690	0.008440975
				0.004580726	0.007871273	0.008530337
				0.005516699	0.0095455956	0.010356537
Sediment	5.1991	19.2393	8.8411	0.016374887	0.029520707	0.031454921
				0.014147617	0.026227224	0.028034256
				0.014406361	0.027163137	0.029101887
				0.017721045	0.034399170	0.036979010

At the basin, a complex mode transformation of the Rayleigh wave can be observed. An incident Rayleigh wave wavelet has caused reflected Rayleigh wave, diffracted body waves in both the basin and the rock and the difference modes of the transmitted Rayleigh wave. The initial arrivals of the Rayleigh waves in basin are horizontally polarised since amplitude of the horizontal component is more than the vertical component. Whereas late arrivals of the Rayleigh waves in basin are vertically polarised since amplitude in the vertical component is greater than the horizontal component. Overall, drastic amplitude amplification of Rayleigh wave just near the basin edge as well as dispersion of the Rayleigh waves can be observed. The reflected slow moving Rayleigh waves from the right edge of the basin can be observed. It appears that the amplitude amplification of the horizontal component is more than that of the vertical component. There is very large increase of duration of Rayleigh wave in the basin due to multiple reflections, development of different modes of Rayleigh waves and the dispersion of the Raleigh waves.

Figure 7 shows the spectral amplitudes of the horizontal and vertical component at different locations both on the rock and the basin. An analysis of figure 7 depicts an

increase of spectral amplitude of both the components of the Rayleigh waves in basin. Overall, the spectral amplitudes are larger in the vertical components than the horizontal components. The decrease of spectral amplitude of the Rayleigh at a faster rate can be observed in the basin due to sediment damping effects. The lowest spectral amplitude of Rayleigh wave can be seen on 750 m right side of centre of the basin

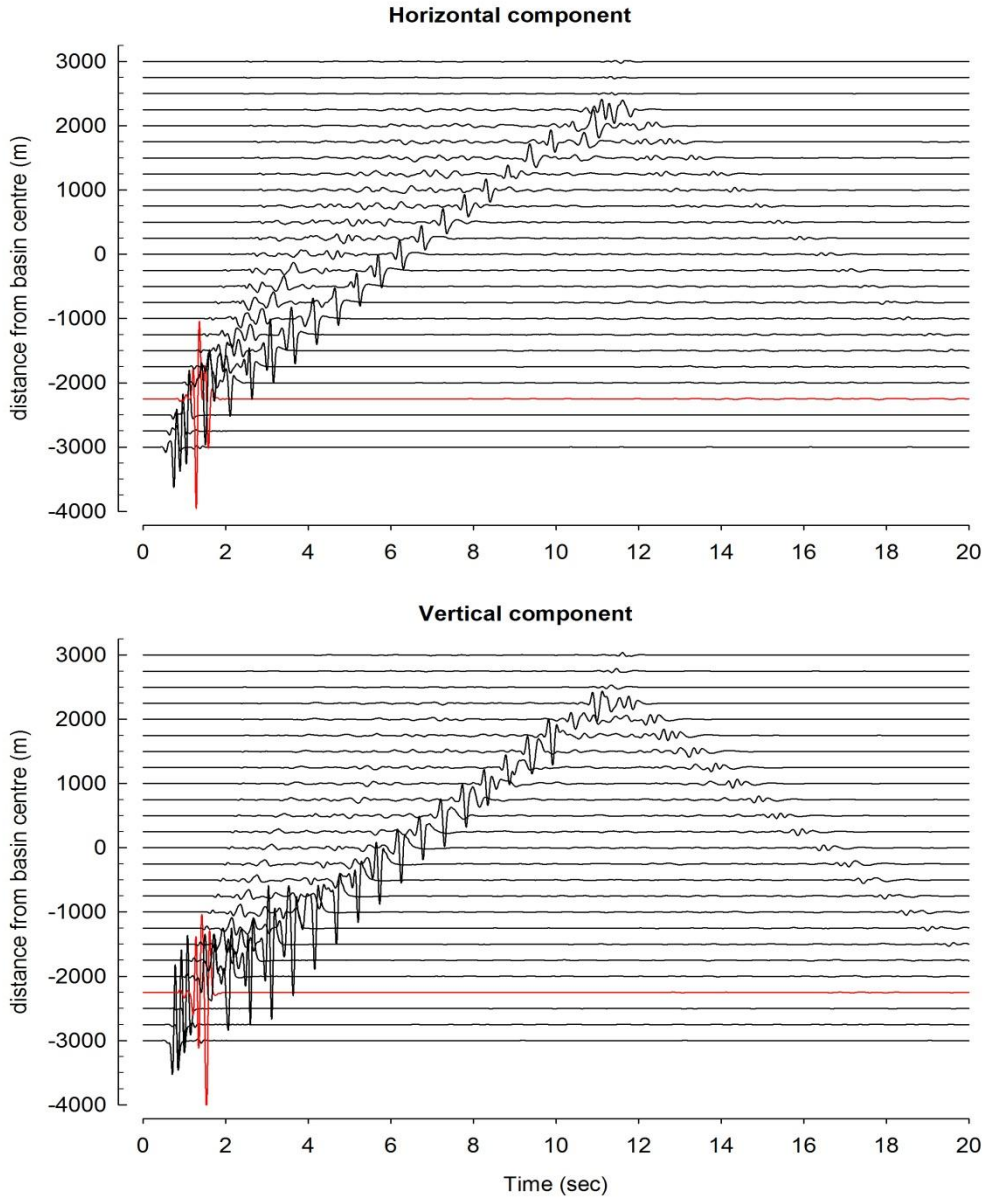

Fiure.3.5 Seismic Response of BTR-waves recorded on 25 receiver stations in the elliptical basin.

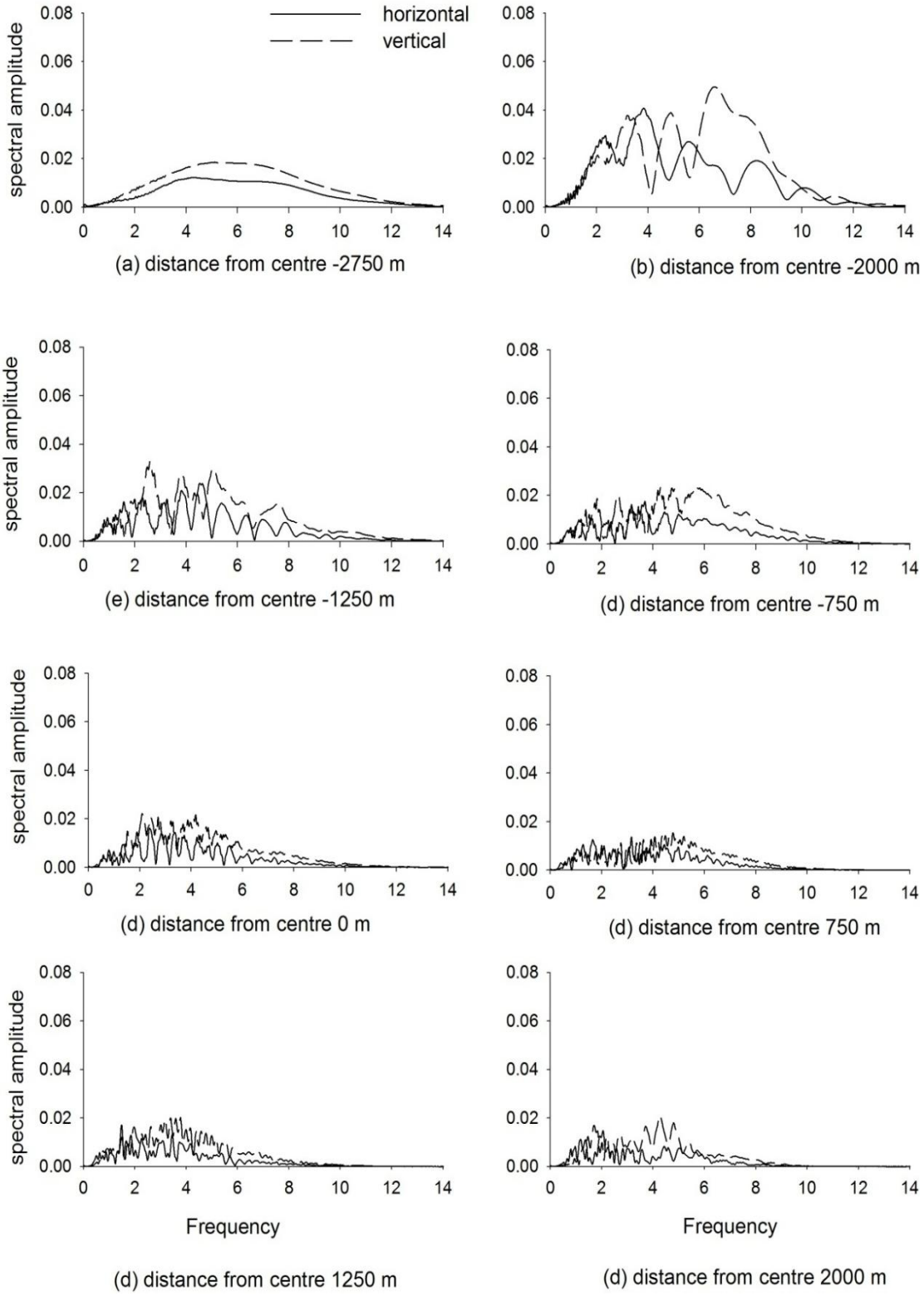

Figure 3.6 Spectral amplitude of both components of Rayleigh waves recorded at different distances from centre of basin of 600 m depth.

3.2.1 Snapshots of BTR-waves in the basin

To see the complex mode transformations and the behaviour of the basin transduved Rayleigh waves snapshots of the waves at different time interval was generated. The snapshots were generated over a length of 1600 m starting from 500 m before the basin and extending over the entire length of the basin. The snapshots were generated after every 0.3 sec. In the figure snapshots after 1.9 sec, 2.8 sec, 3.4 sec, 4 sec, 4.6 sec, 5.5 sec is shown for both the horizontal and vertical component.

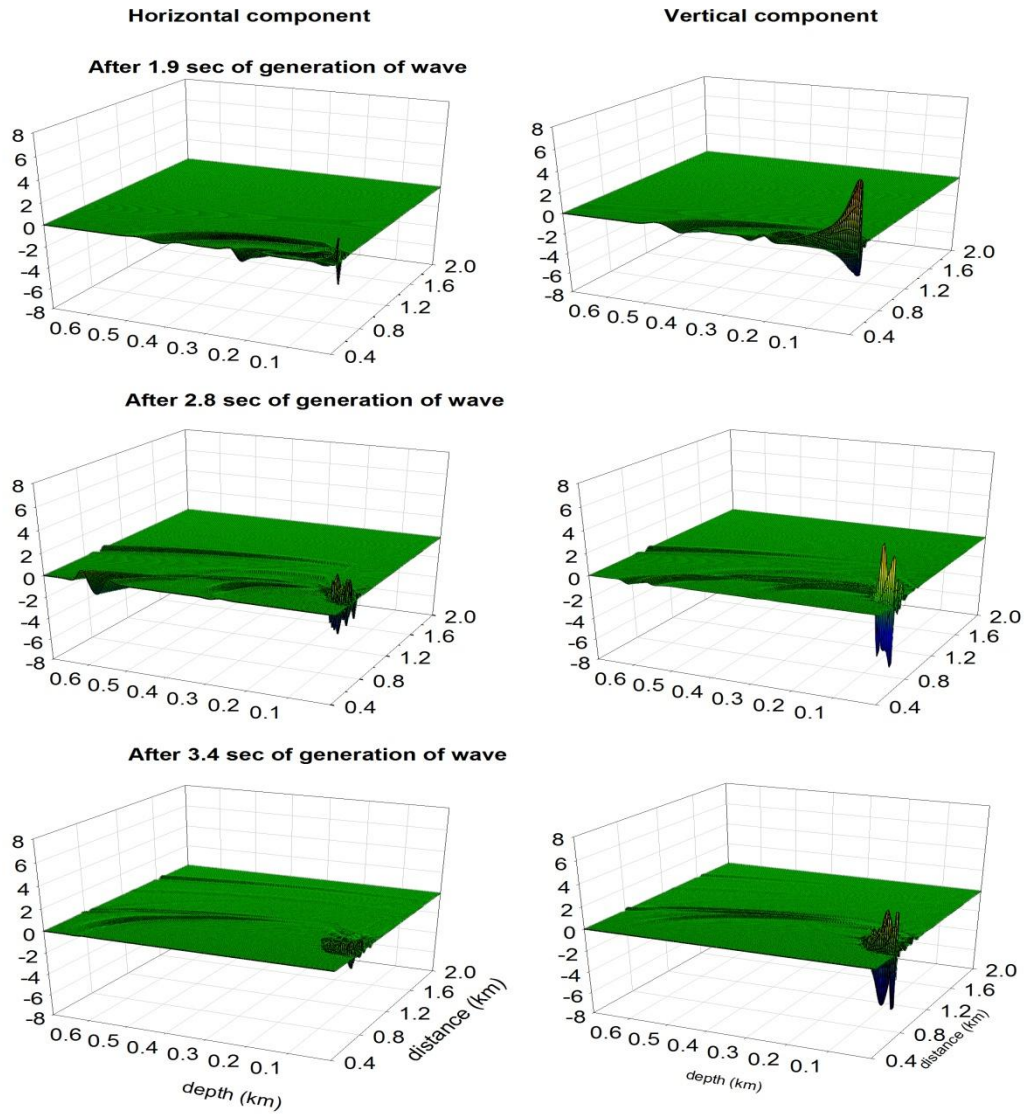

Figure 3.7 Snapshot showing the travel path of BTR-waves.

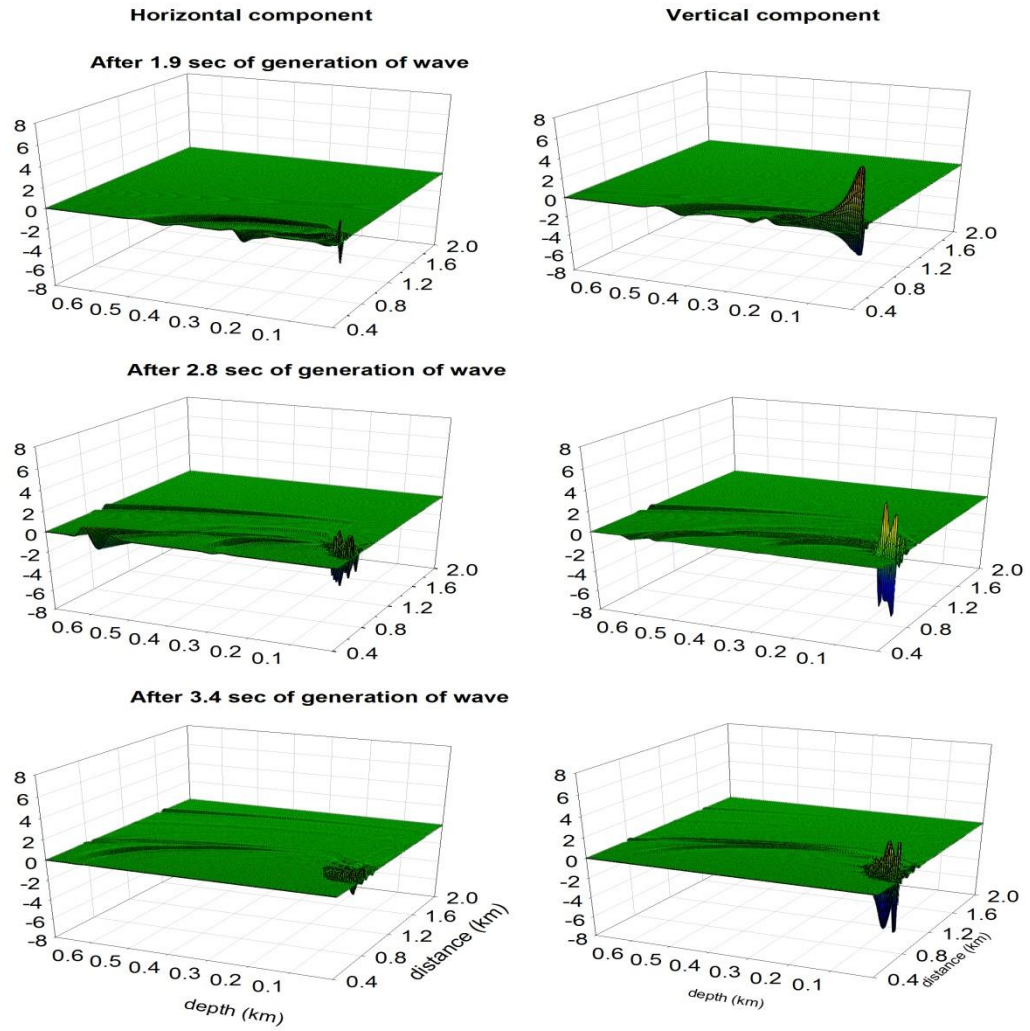

Figure 3.8 Snapshot showing the travel path of BTR-waves.

Analysis of the figures shows the travel path of the Rayleigh wave and its behaviour in the basin. As the waves enter into the basin they get amplified. At very early stage of time the effect of waves is seen only near the edges. After 2.8 sec the waves seem to affect the entire basin. As the waves moves further their amplitude decreases due to the damping in the basin. The dispersion of the waves can be seen along the depth of the basin in the earlier arrivals. It is also observed that due to the constructive interference the vertical component decreases and increases with time. The wave can be seen leaving the basin. The amplitude of vertical components is seen higher than the horizontal component.

CHAPTER # 4

STUDY OF EFFECTS OF SHAPE-RATIO AND SHAPE OF BASIN ON THE BTR-WAVES

4.1 INTRODUCTION:

A lot of research work has already been done on the body wave amplification in the basin but very limited work has been done on surface waves, although surface waves can cause severe damage as compared to the body waves. The rock surrounding the basin can also cause different amount of amplification in the basin since the impedance contrast will change at the basin edge. To avoid structural damages due to the basin, the quantification of the effect of basin on the mode transformation of basin transduced waves is necessary.

The existence of basin transduced surface waves were first analysed during the 1971 San Fernado Californa earthquake by Hanks (1975). Amplification of Rayleigh waves takes place in the basin depending upon the thickness of the basin, impedance contrast and the shape of the basin. The shape of the basin can affect the amplification near the basin edges. Narayan(2010) reported that the largest value of spectral amplification of the Rayleigh waves in the basin depends largely on the fundamental frequency of the basin. In the following sub sections detailed elaboration of effects of basin-shape-ratio and shape of basin has been discussed.

4.2 EFFECT OF BASIN-SHAPE-RATIO ON BTR-WAVES:

The seismic response of the basin with varying shape-ratio was computed to study the effects on the dispersion characteristics and the complex mode transformations of the Rayleigh waves. For this purpose an elliptical basin with varying depth are taken. The depths of the basins are 100m, 200 m, 300 m, 400 m , 500 m and 600 m and the width is taken as 5000 m (5 km). So, the shape ratio for basins having depth as 100m, 200 m, 300

m, 400 m , 500 m and 600 m is 0.04, 0.08, 0.12, 0.16, 0.2 and 0.24 respectively. The source is taken at 100 m depth and 1100 m away from the boundary (Fig. 4.1). Total 25 stations at a distance of 50 m are incorporated in the model. The receivers are extended to a distance of 6000 m. The first receiver is kept at a distance of 900 m from the source. The source and the receiver position are same for all the models. The time step taken is 0.001 sec. The aim is to examine the BTR wave characteristics, reflection of Rayleigh wave from edge of the basin and the dispersion characteristics. Figures 4.2- 4.7 show the horizontal and vertical components of seismic responses of basins with depths as 100m, 200 m, 300 m, 400 m , 500 m and 600 m, respectively.

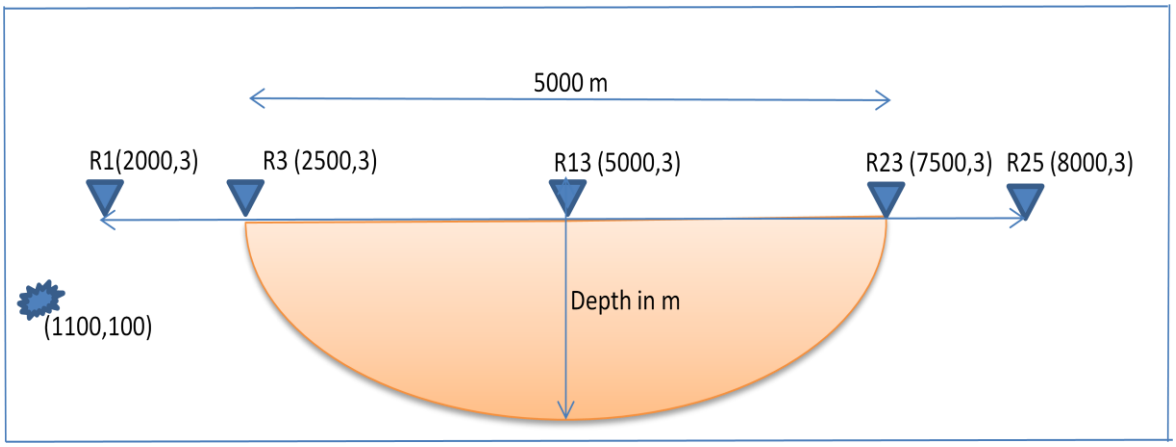

Figure 4.1 Elliptical basin model for analysis of basin depth effects.

The analysis of figures 4.2-4.7 depicts that the as the basin depth increases the dispersion and duration of BTR waves increases with increase of depth of basin. Further, there is tremendous effects on the amplitude of different models of the BTR-waves. For example, the amplitude of the horizontally polarised fast moving mode of BTR-wave is decreasing with an increase of depth of basin. In contrast to this, the amplitude of the vertically polarised slow moving mode of BTR-wave is increasing with an increase of depth of basin. Further, an increase of reflection of the BTR-waves with an increase of depth of basin can be inferred. We can clearly see the later arriving waves near the basin edge in all the cases which are the surface waves. The amplification is larger in the case of lesser soil thickness near the basin edge.

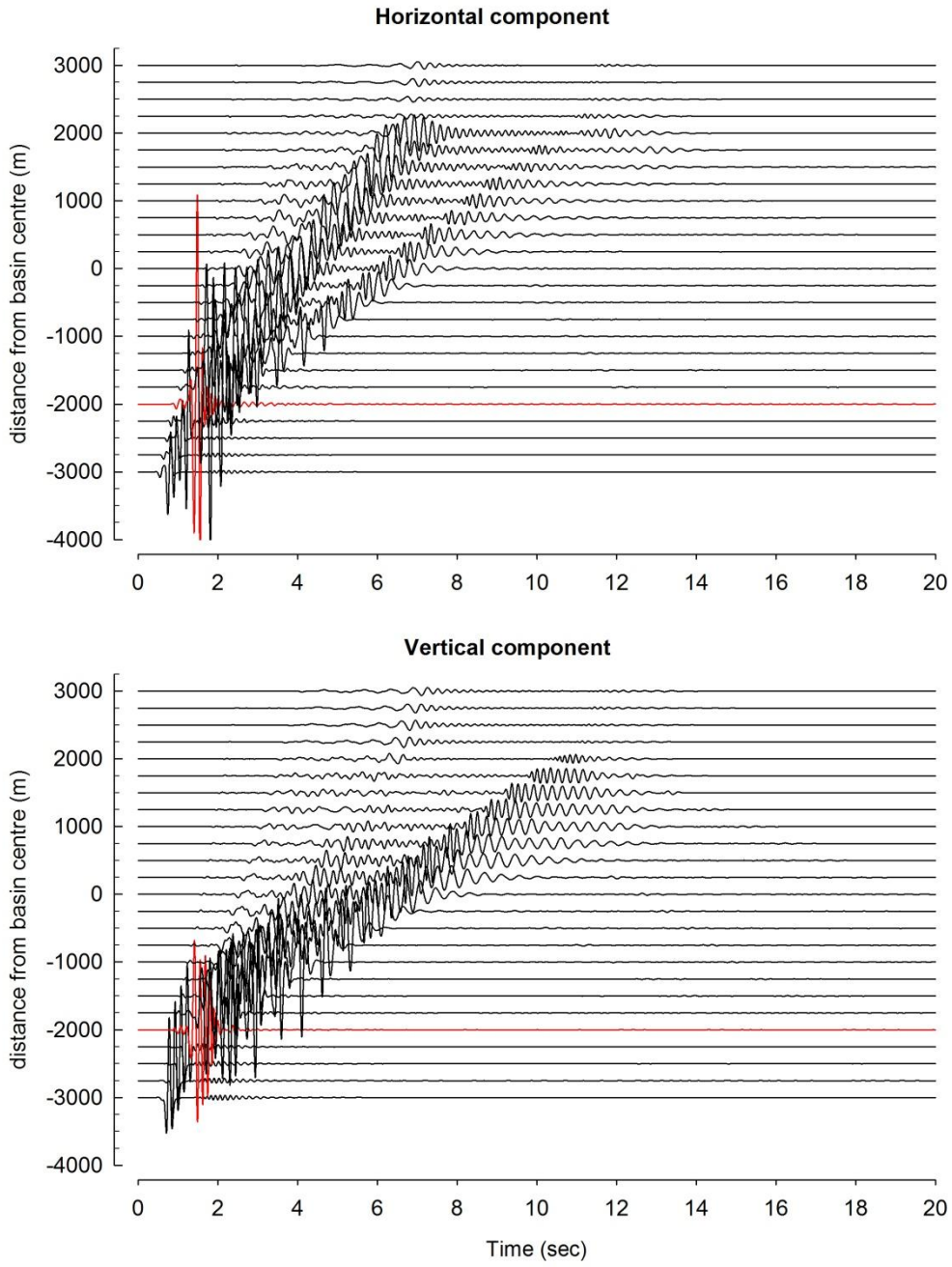

Figure 4.2 Seismic Response of BTR-waves recorded on 25 receiver stations in the elliptical basin for 100 m depth.

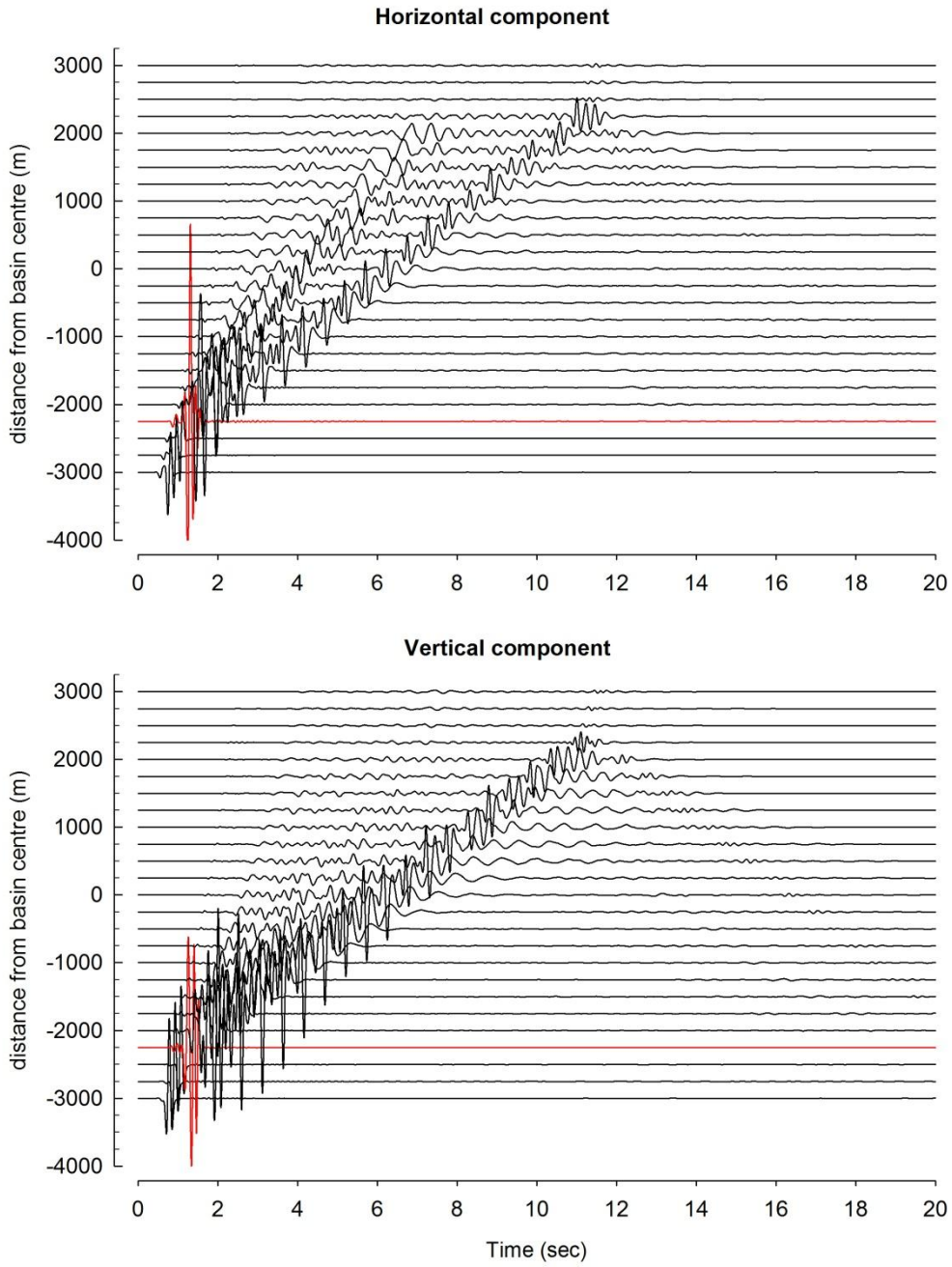

Figure 4.3 Seismic Response of BTR-waves recorded on 25 receiver stations in the elliptical basin for 200m depth.

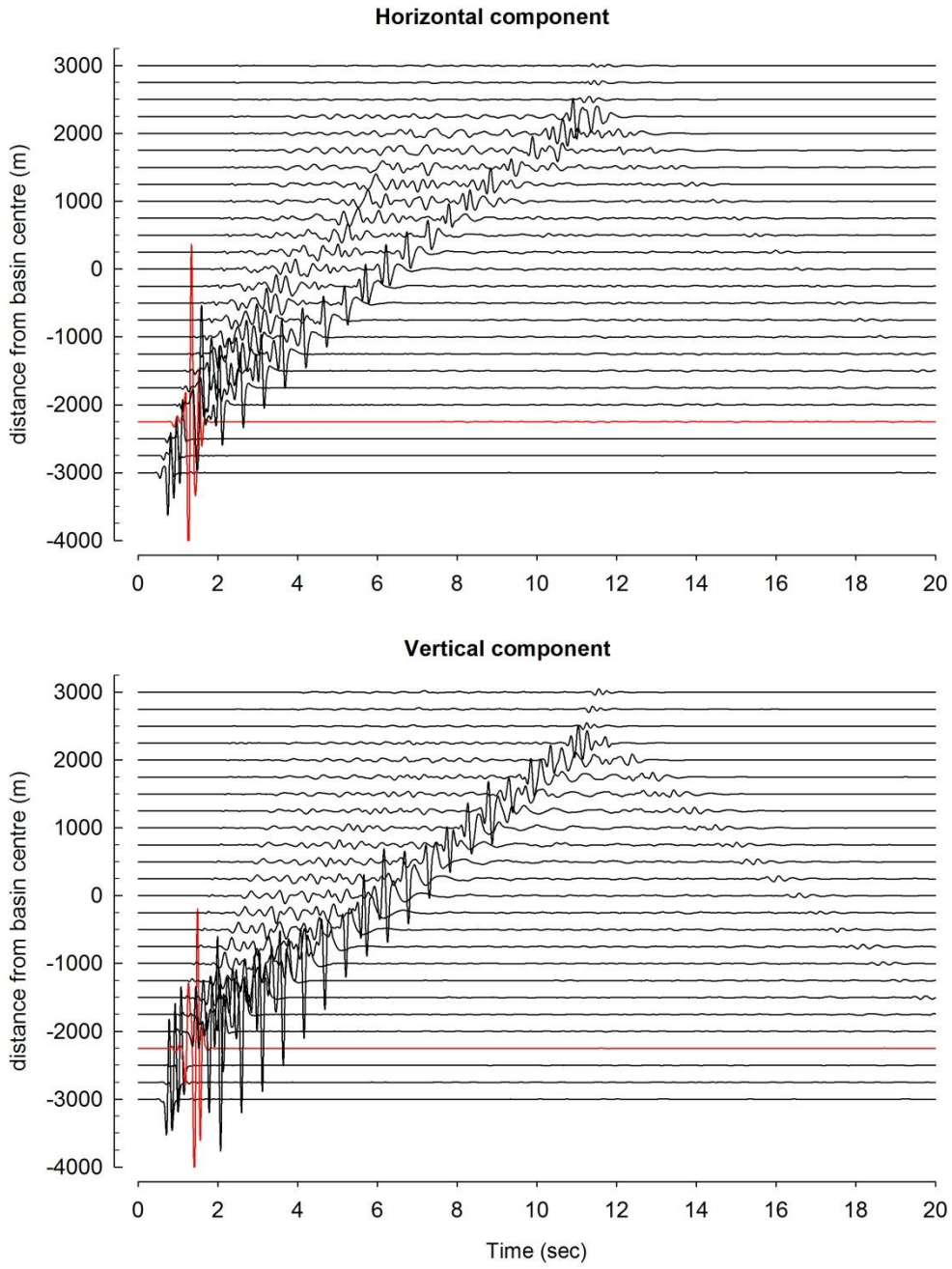

Figure 4.4 Seismic Response of BTR-waves recorded on 25 receiver stations in the elliptical basin for 300 m depth.

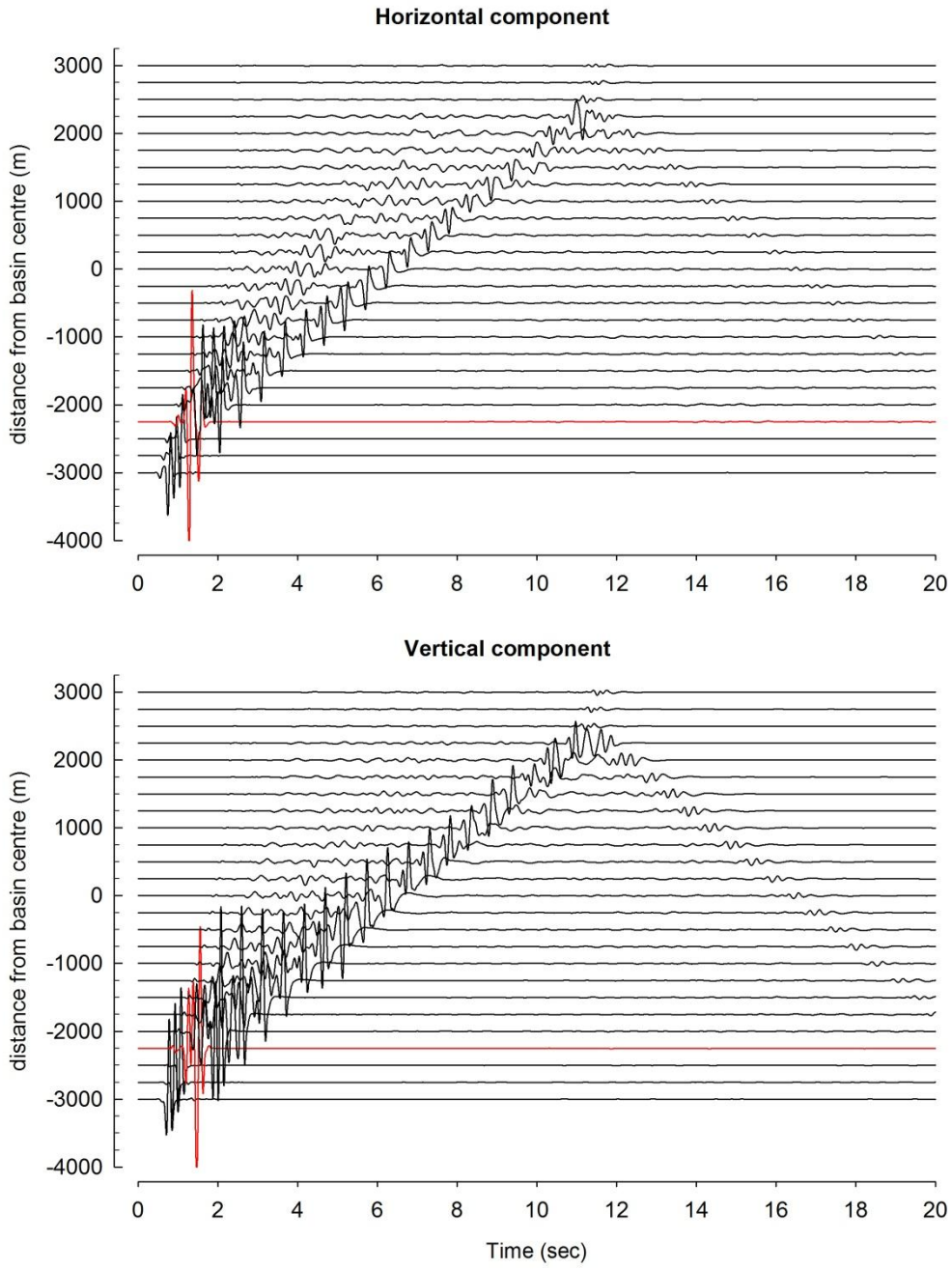

Figure 4.5 Seismic Response of BTR-waves recorded on 25 receiver stations in the elliptical basin for 400 m depth.

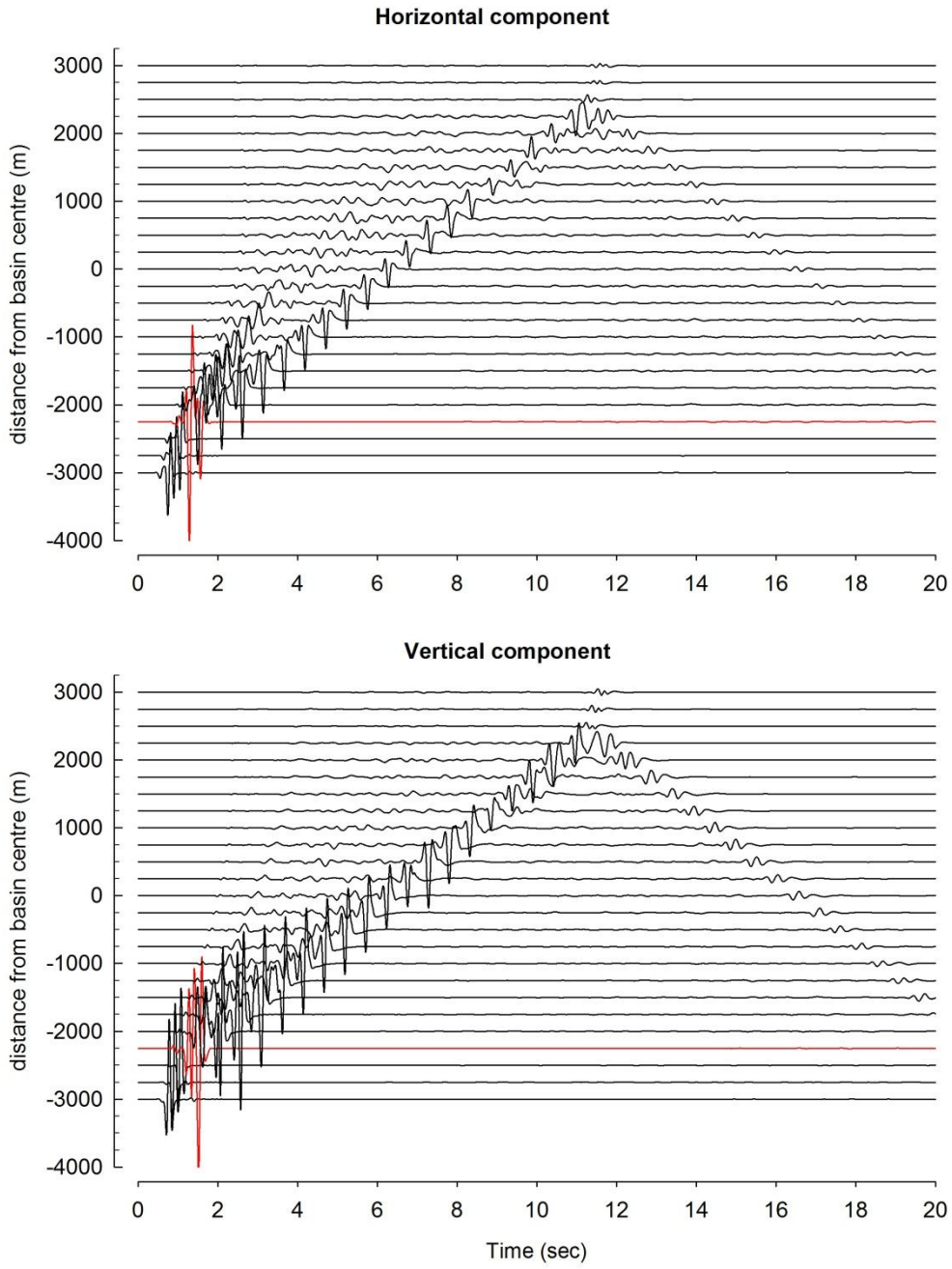

Figure 4.6 Seismic Response of BTR-waves recorded on 25 receiver stations in the elliptical basin for 500 m depth.

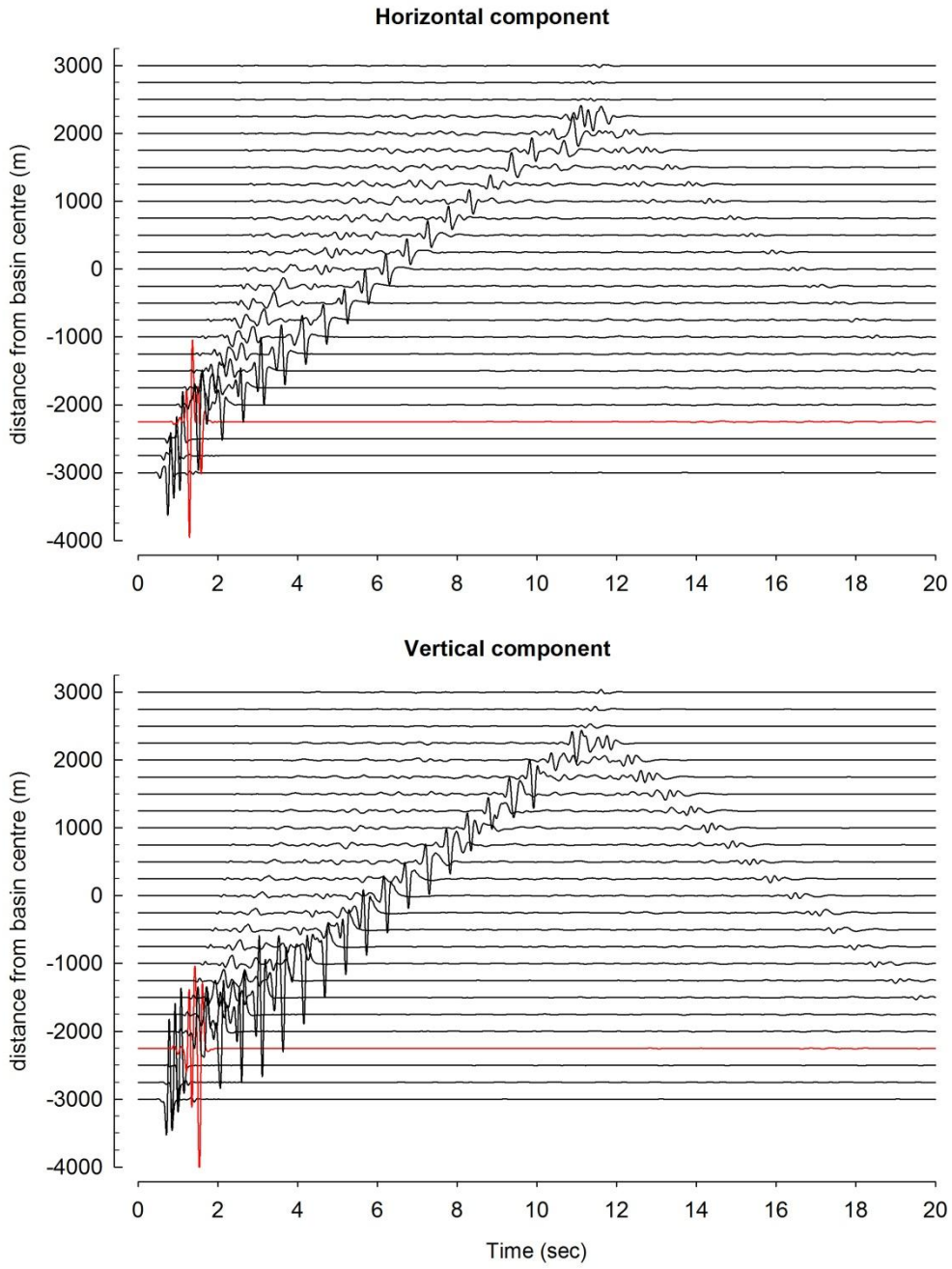

Figure. 4.7 Seismic Response of BTR-waves recorded on 25 receiver stations in the elliptical basin for 600 m depth.

The earlier arrivals in the basin are found to be less dispersed than the later arrivals. The highest peak is seen in the case of lower depths of 100 m and 200. We can also see that as we moved further along the basin edge the wave became vertically polarized. The peak amplitude of Rayleigh wave was found to vary according to the constructive interference of waves near the basin edges. The amplitude is found to decrease near the basin edges as the depth increases. A comparison of amplitudes of BTR-waves in the horizontal and vertical components at station which towards the left and at a distance of 1250 m from the centre of basin is shown in figures 4.8. A drastic change in the characteristics of BTR-waves with an increase of depth of basin can be inferred.

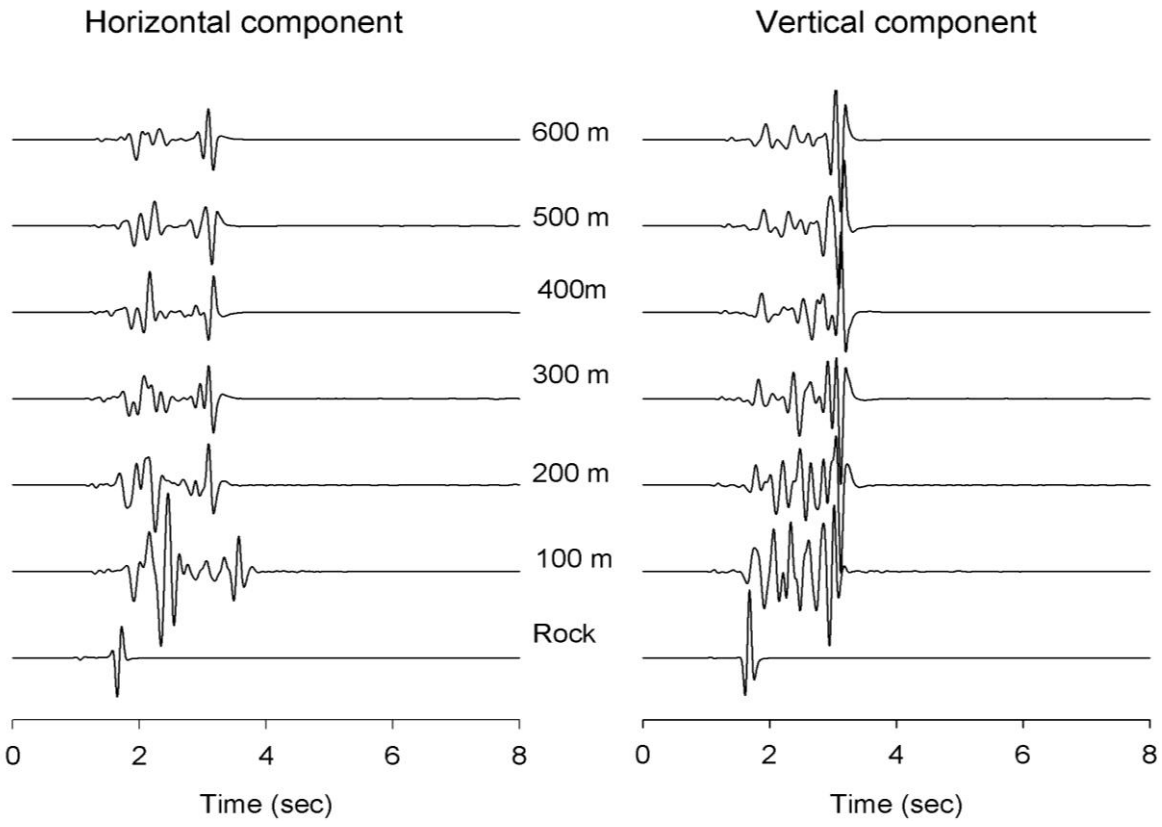

Figure 4.8 Comparison of spectral amplitude of BTR wave recorded at 8th station (1250 m left of the centre of basin).

4.2.1 Effects of shape-ratio on spectral amplification

The spectral amplification computed at 8 stations with respect to the centre of basin are shown in figure 4.9 to 4.14. The stations used are located at a distance of 2.75 km, 2 km, 1.25 km, 0.75 km left from the centre of basin, one station at basin and three stations at a distance of 0.75 km, 1.25 km, 2 km right of the centre of basin. As the depth increases from 100 to 600 m the largest value of the spectral amplification shifts towards the lower frequency in case of both the horizontal and vertical components. The amplification is high in case of horizontal component. The spectral amplification is upto 9 times in case of 400 m depth basin at very low frequency. At higher frequency the spectral amplification decreases as the depth increases in case of horizontal component. Towards the end of the basin the largest peak is obtained corresponding to the 600 m depth basin.

This largest value then shifts toward higher frequency as the depth increases. The peaks increases as the depth increases. The de-amplification of the vertical component can be seen corresponding to the highest amplification of the horizontal components. Wiggling of waves can be seen increasing as the depth increases which may be due to the dispersive nature of the Rayleigh waves. The shape of spectral amplification is varying largely from the basin edge as the depth increases. Due to the dispersive nature of Rayleigh waves and damping in the basin the amplification curve is smoother for higher depth of basin. The highest amplification of the horizontal component of Rayleigh waves went as high as 11 which can be seen corresponding to 300 m depth, and at a distance of 1250 m right of the centre of basin this high value towards the end of the basin may be due to the reflections from the edge of the basin.

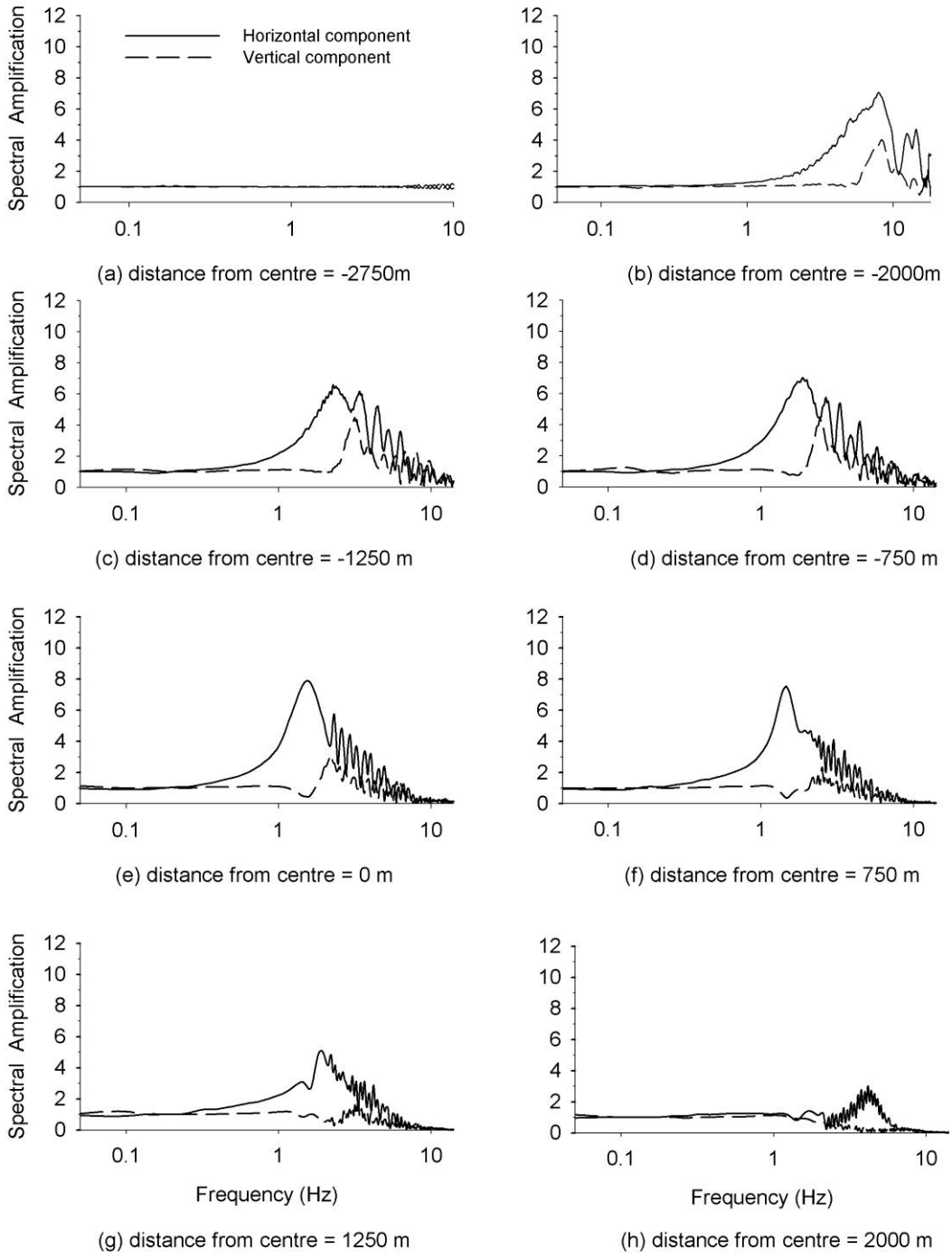

Figure 4.9 BTR waves spectral amplification for 100 m basin depth.

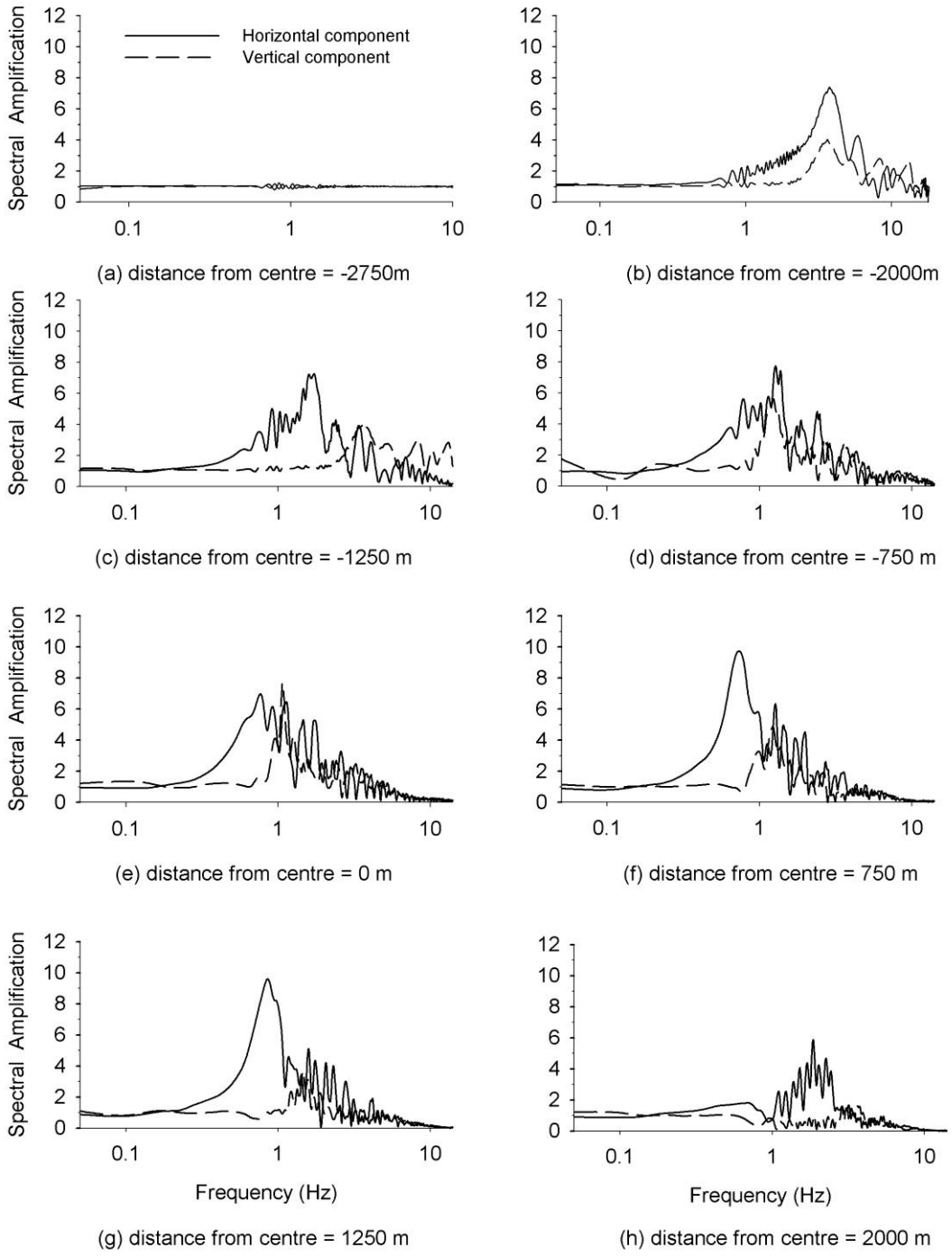

Figure 4.10 BTR waves spectral amplification for 200 m basin depth.

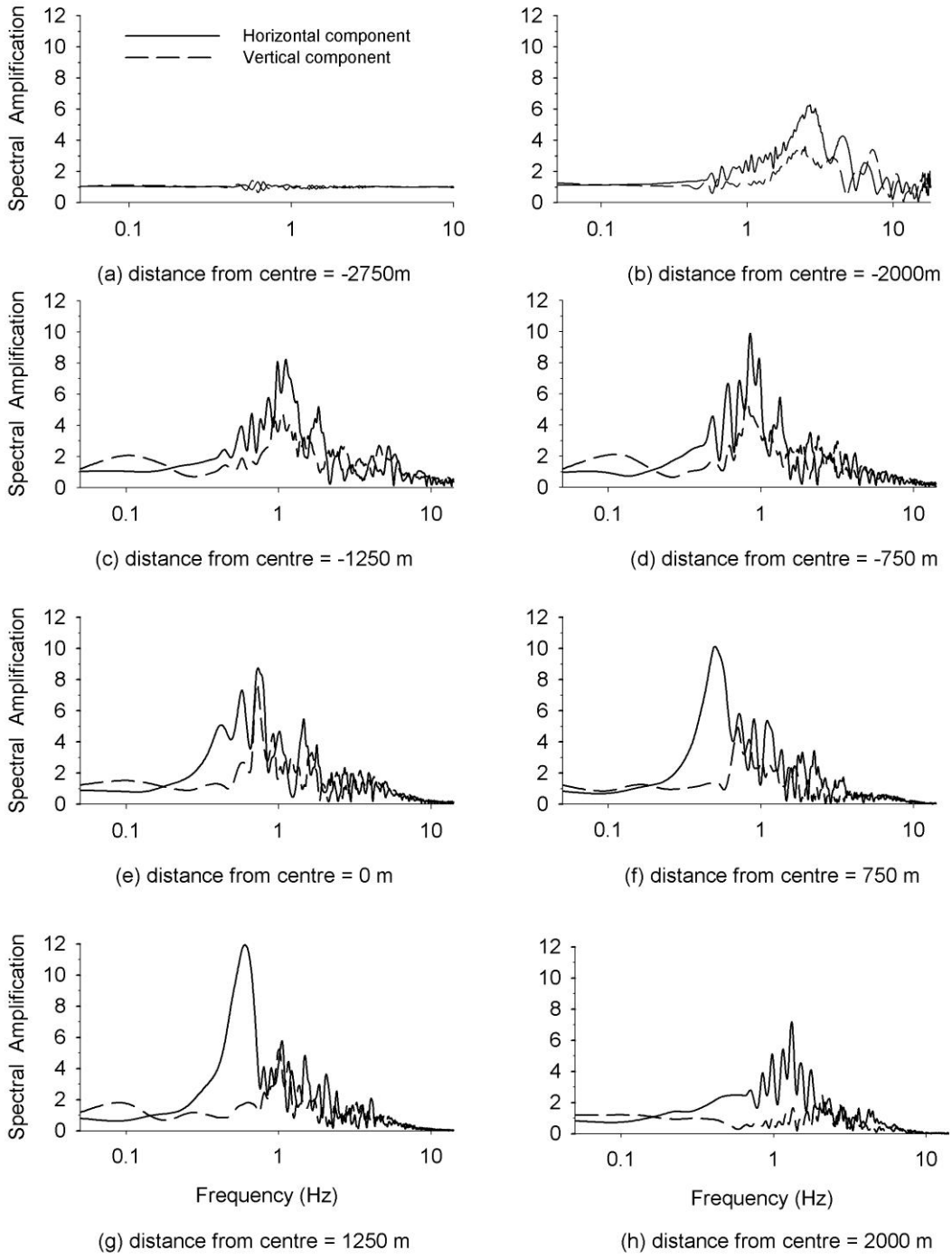

Figure 4.11 BTR waves spectral amplification for 300 m basin depth.

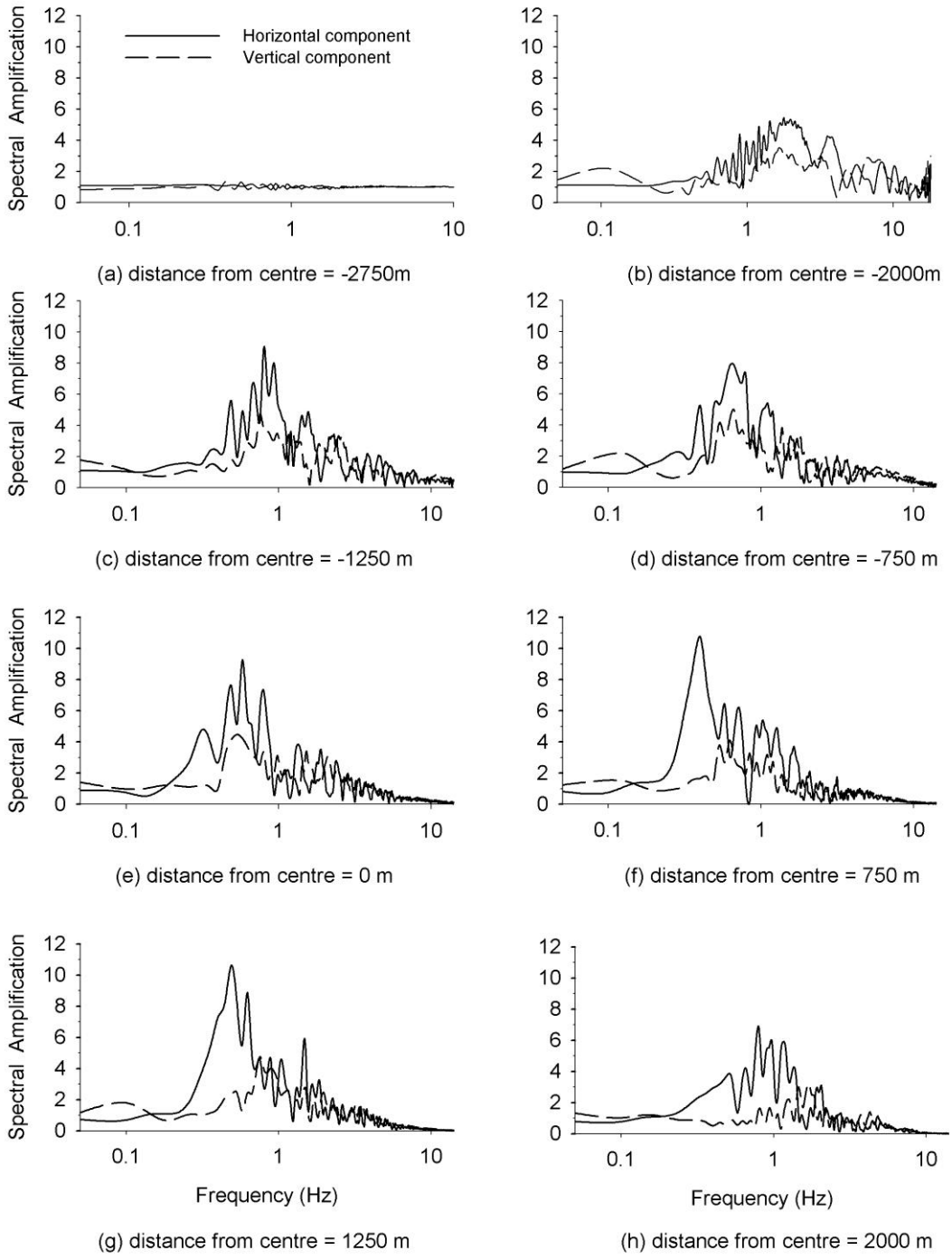

Figure 4.12 BTR waves spectral amplification for 400 m basin depth.

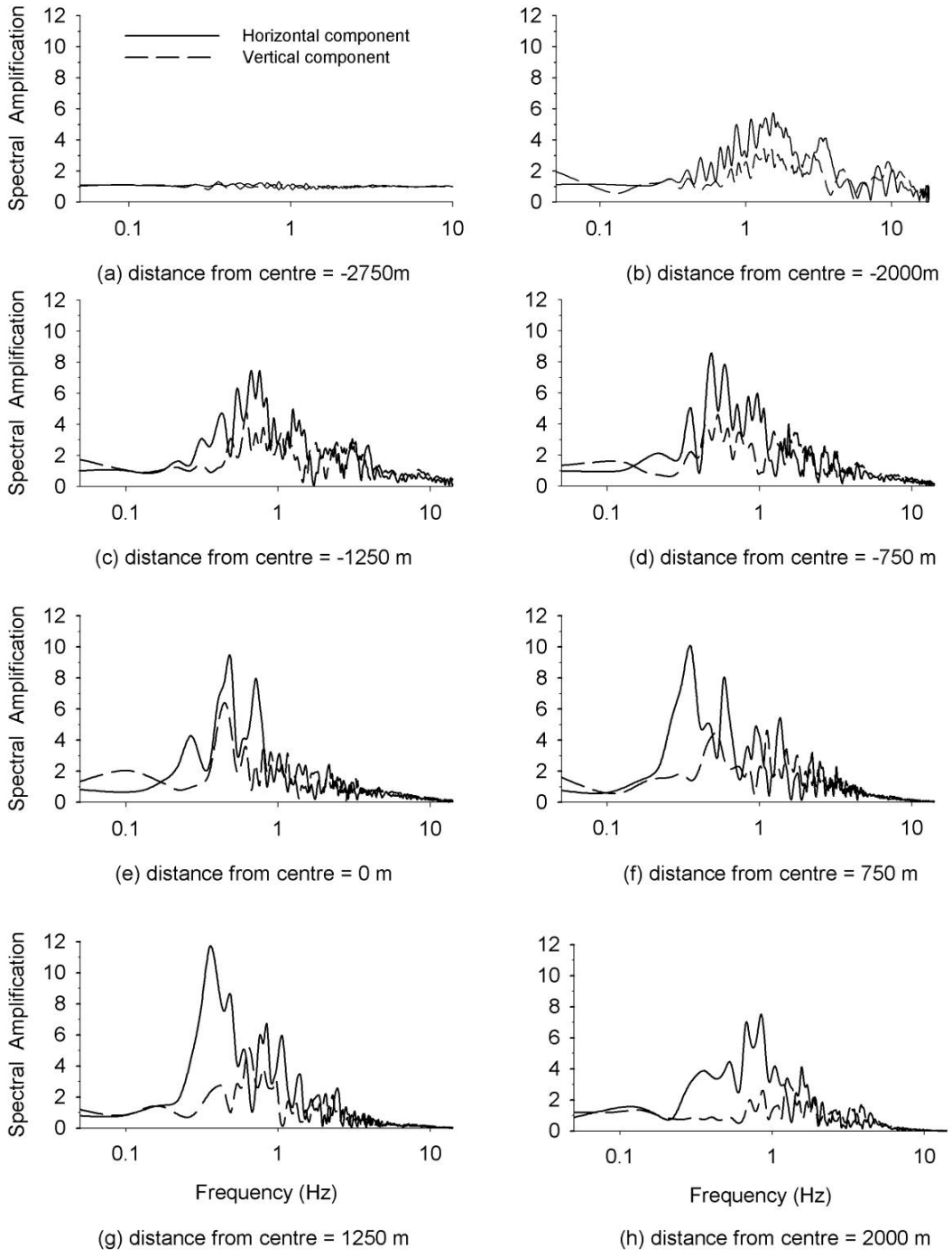

Figure 4.13 BTR waves spectral amplification for 500 m basin depth.

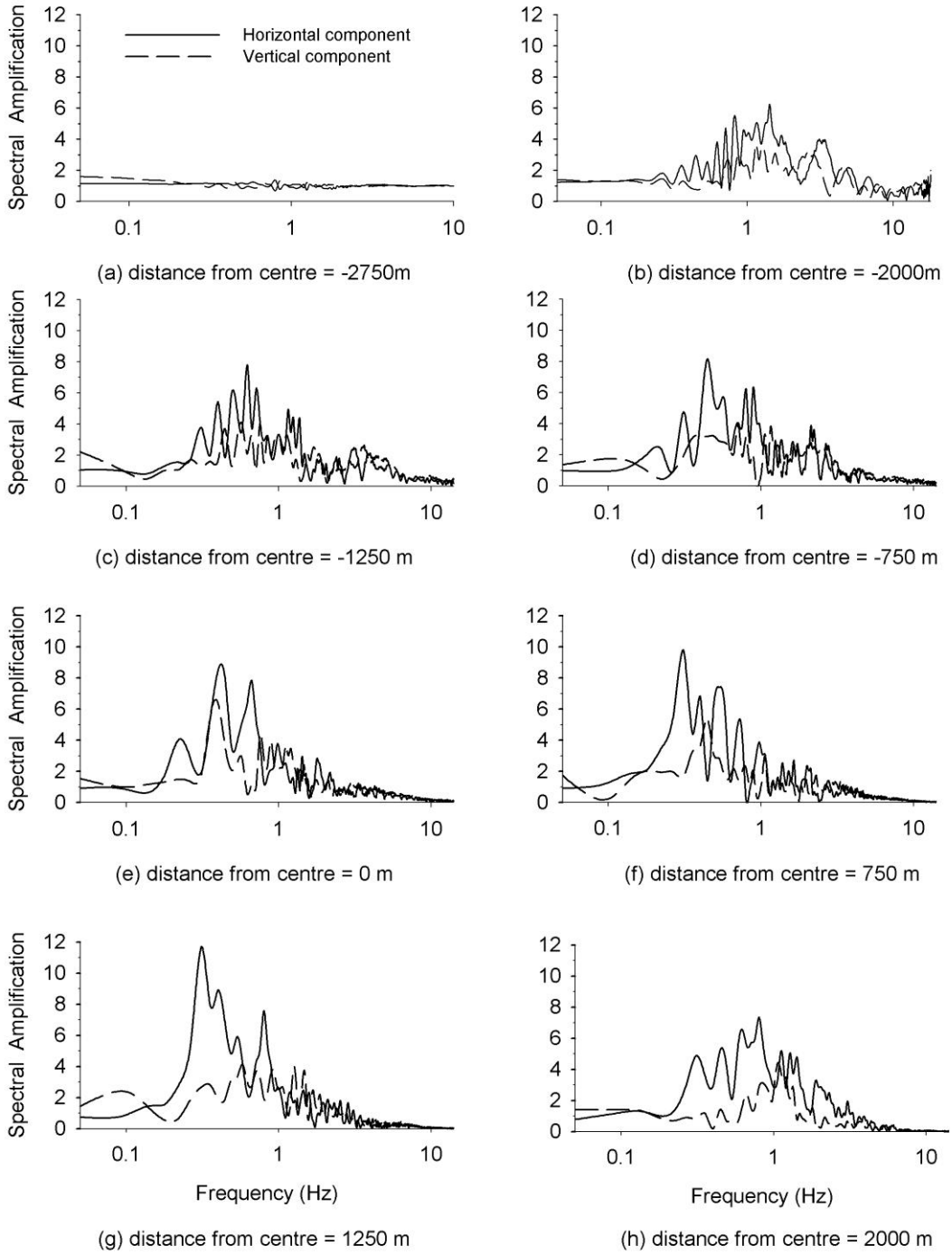

Figure 4.14 BTR waves spectral amplification for 600 m basin depth.

.

The comparative study of spectral amplification is carried for 100m, 200m 400m and 600m depth for the 8th station (1250 m left from the centre of basin) and is shown in figure 4.15. The analysis of this results showed that spectral amplification varies with basin depth to a very large extent. The value of order 9 was found in case of 400 m basin depth for very low frequency near the edge of the basin. Spectral amplification seems to increase as basin depth increase for lower frequencies whereas it decreases with depth at higher frequencies.

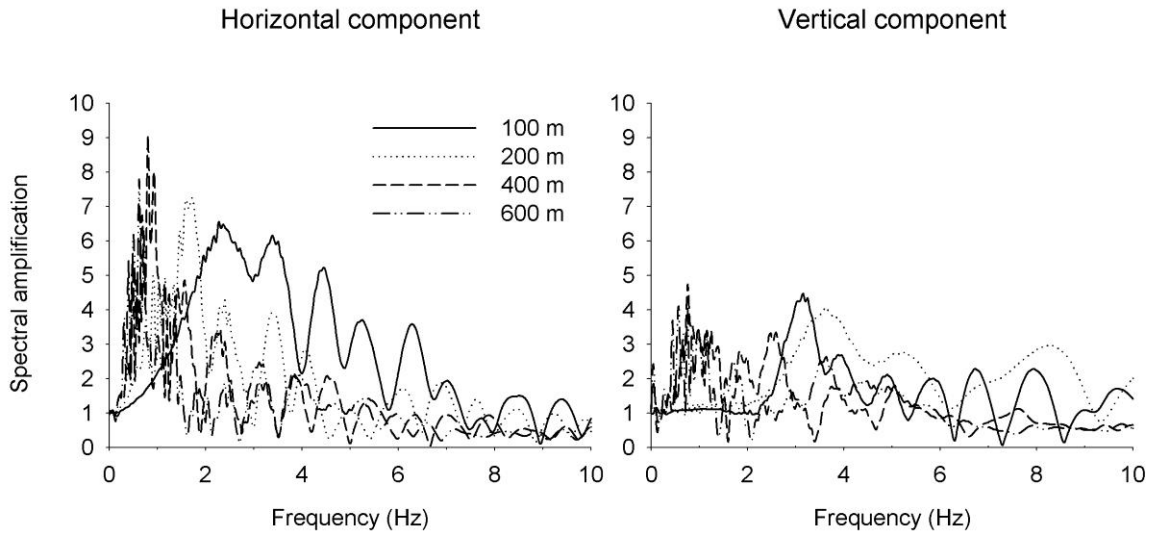

Figure 4.15 Spectral amplification for different soil thickness corresponding to 8th station (1250 m left from the basin centre).

4.2.2 Average spectral amplification of BTR wave

The average spectral amplification of the BTR waves was computed and is shown in figure 4.16. The analysis of the figure shows that for 100 m depth the average spectral amplification is of the order 4 for horizontal component. The ASA value for horizontal component is quite higher than the vertical component in case of 100 depth. As the depth increases the value of ASA reduces to nearly 1 around the centre of basin and further reduces afterwards. The average spectral amplification values of horizontal and vertical components are nearly same for higher depths of basin.

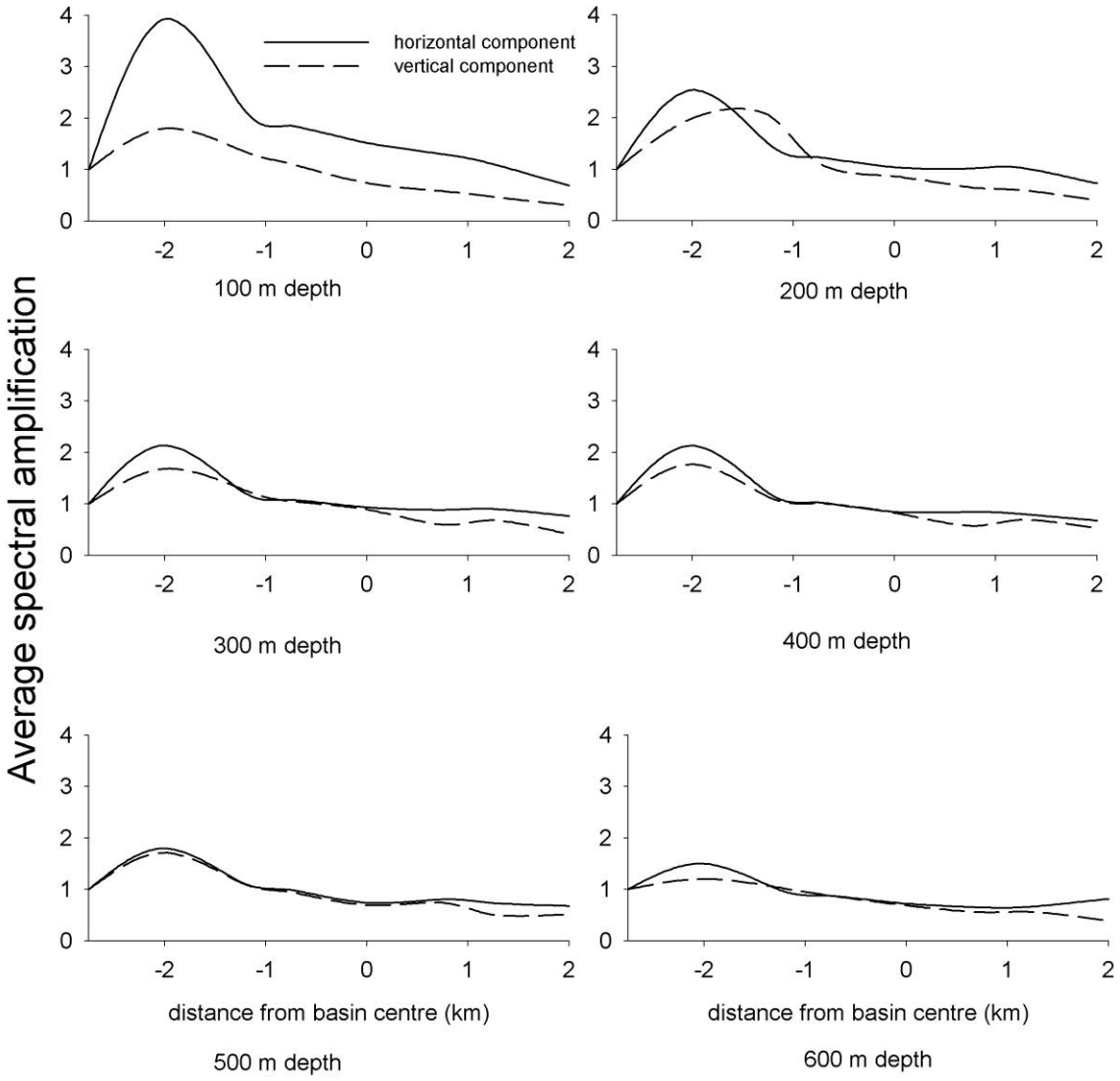

Figure 4.16 Average spectral amplification of BTR waves of different basin depths.

4.3 EFFECT OF BASIN SHAPE ON BTR-WAVES

To see the effect of various shape of basin on the BTR waves 4 shapes elliptical (MS1 model), trapezoidal with edge slope 20^0 (MS2), trapezoidal with edge slope 45^0 (MS2) and triangular basin (MS4) were taken for same basin depth as shown in figure 4.17. The horizontal and vertical components of the seismic responses of all the models MS1 to MS4 were computed as shown in the figures 4.18-4.21.

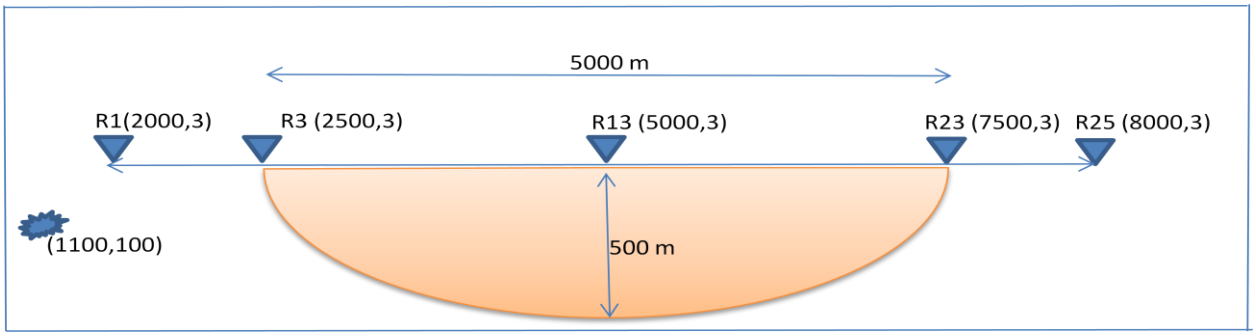

(a) CIRCULAR BASIN **(MS1)**

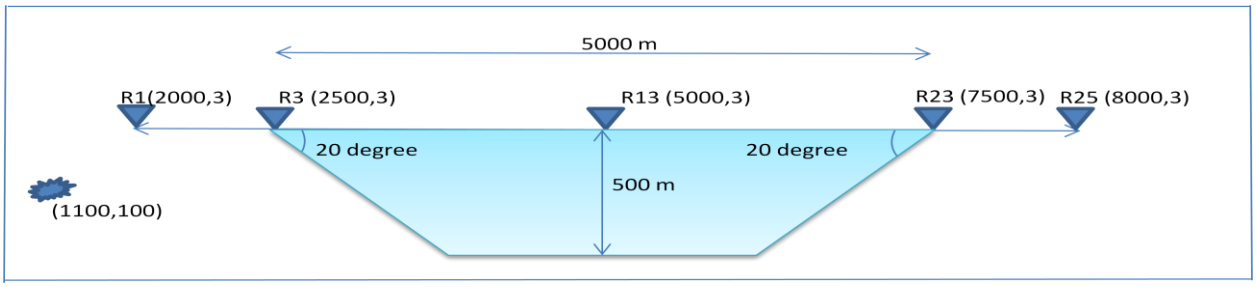

(b) TRAPEZOIDAL BASIN (20 degree) **(MS2)**

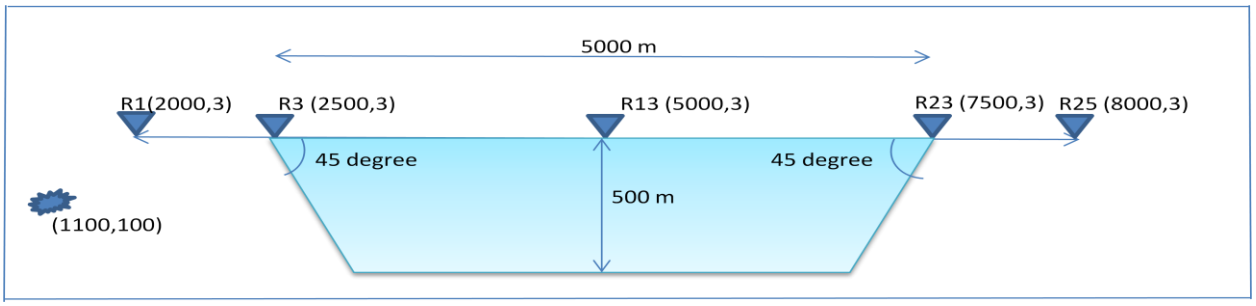

(c) TRAPEZOIDAL BASIN (45 degree) **(MS3)**

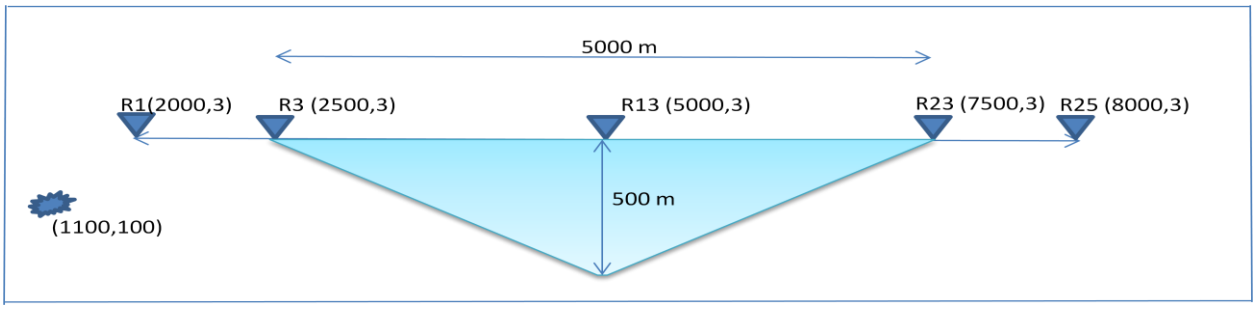

(d) TRIANGULAR BASIN **(MS4)**

Figure 4.17 Shapes of basin with maximum basin depth of 500 m.

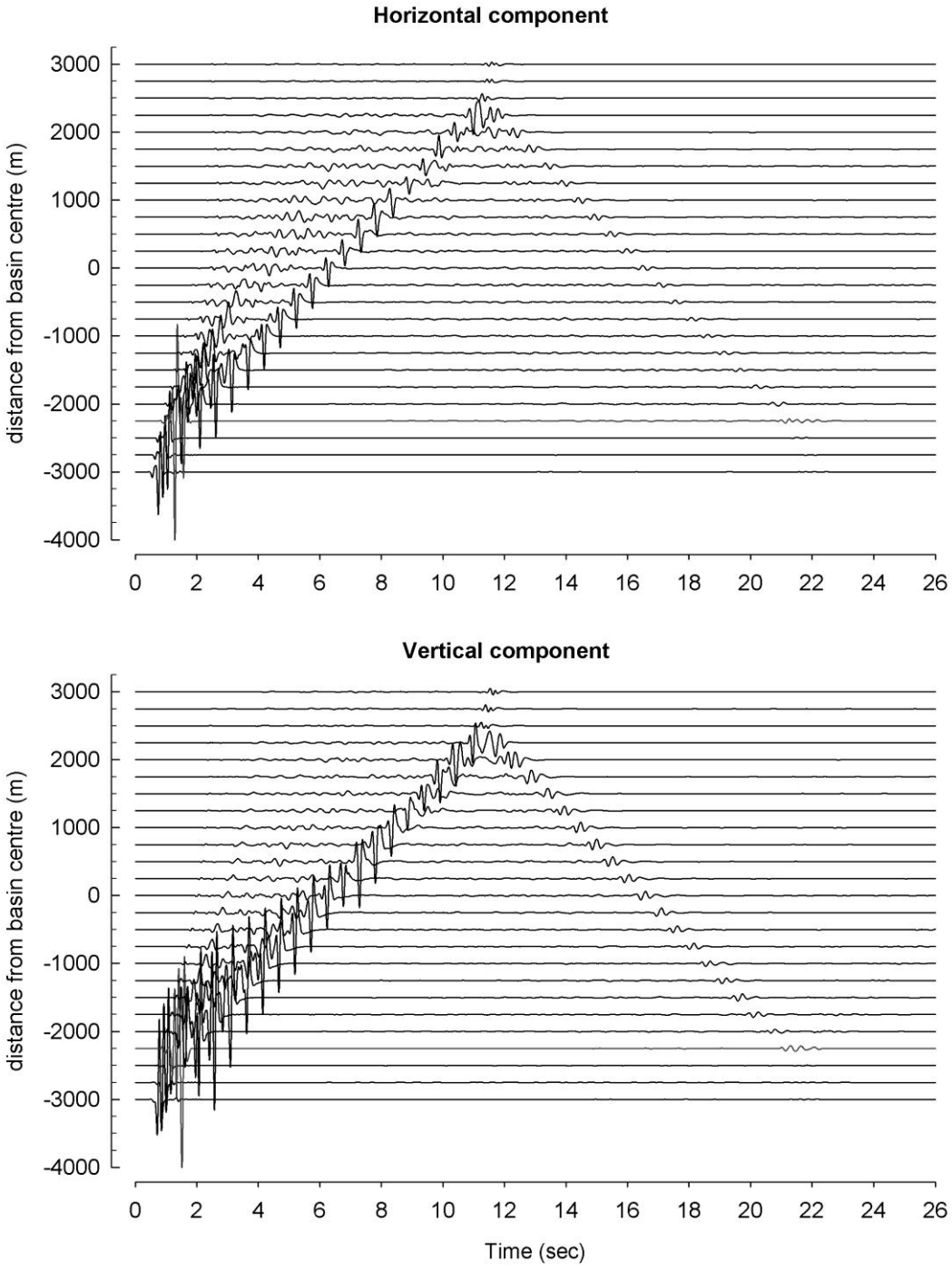

Figure 4.18 Seismic response of BTR waves at 25 stations for model MS1

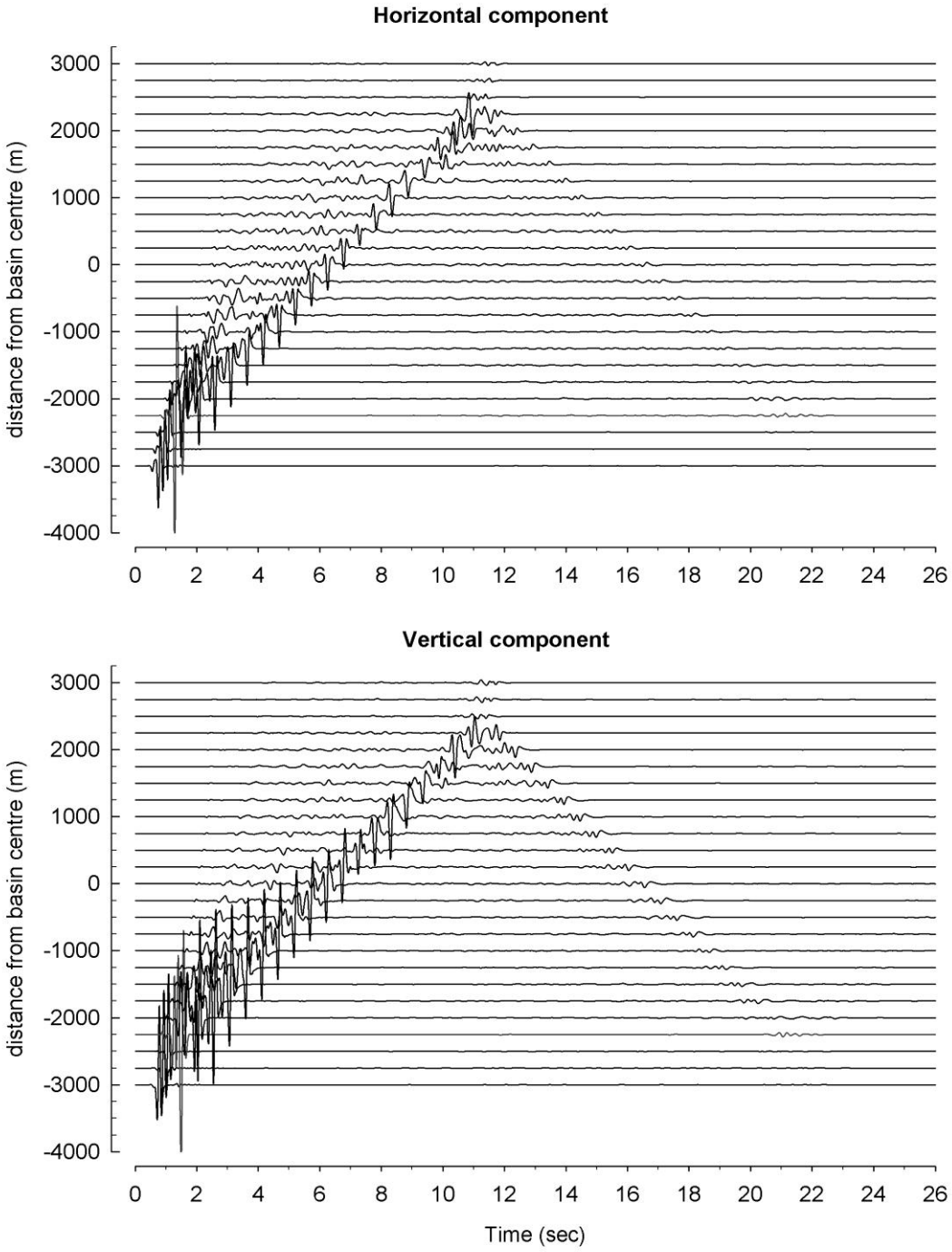

Figure 4.19 Seismic response of BTR waves at 25 stations for model MS2

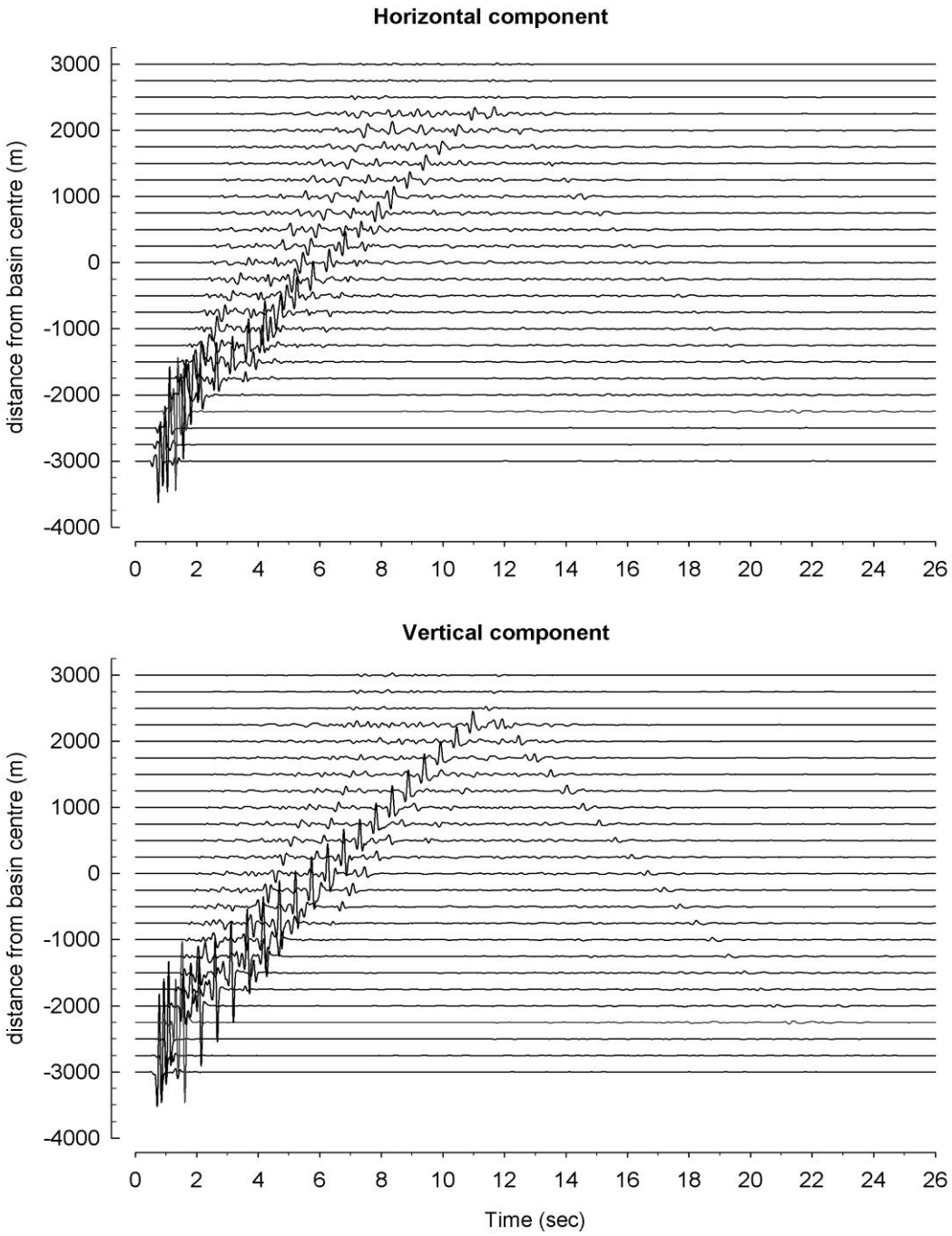

Figure 4.20 Seismic response of BTR waves at 25 stations for model MS3

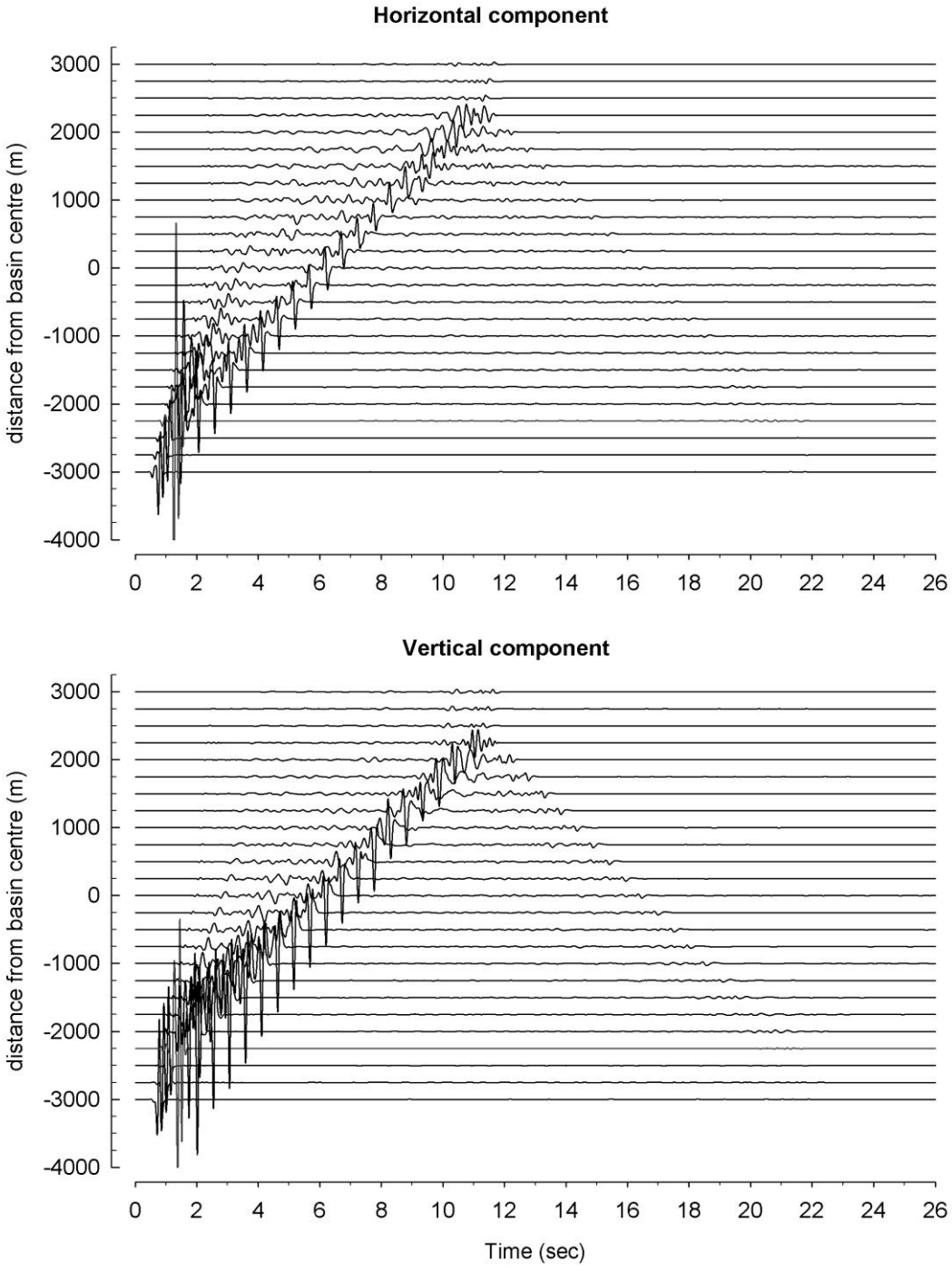

Figure 4.21 Seismic response of BTR waves at 25 stations for model MS4

A lot of change in the amplitude, the dispersion of Rayleigh waves and the duration can be inferred with change of shape of the basin. Various modes of the BTR-waves are seen in the arrivals for the MS3 model and MS4 model. The seismic response of MS1 model was quite similar to MS2,which shows that trapezoidal shape basin with gentle slope behave similar to the elliptical basin. The decrease of amplitude with the distance travelled is higher in case of MS3 and MS4 model but the earlier arrivals of waves showed high amplitude in these models.

4.3.1 Effect of basin shape on spectral amplification

The spectral amplitude of the Rayleigh waves is shown in figures 4.22 -4.25. The largest value of spectral amplitude is corresponding to the MS4 model. There is larger amplification of the horizontal components as compared to the vertical components, particularly in the lower frequency range. In case of very large wavelength of Rayleigh waves (frequency less than 0.1 Hz), there is no amplification of both the components of the BTR-waves. Means, they will be unaffected by the presence of a basin having width 5 km and depth 600 m.

On an average corresponding to the frequency 0.1 to 1.0 Hz, the amplification of horizontal components is much larger to that of the vertical components. In case of frequency larger than 1.0 Hz the amplification of the horizontal and the vertical components are to some extent comparable.

4.3.1 Average spectral amplification of BTR wave

The average value of spectral amplification is computed for both components and shown in the figure 4.26. The analysis showed the variation in the value of ASA varied with the change in shape a lot, particularly in the horizontal component. The largest value of spectral amplification of the horizontal component is seen corresponding to the MS4 model that is triangular in shape of the order 2.1.

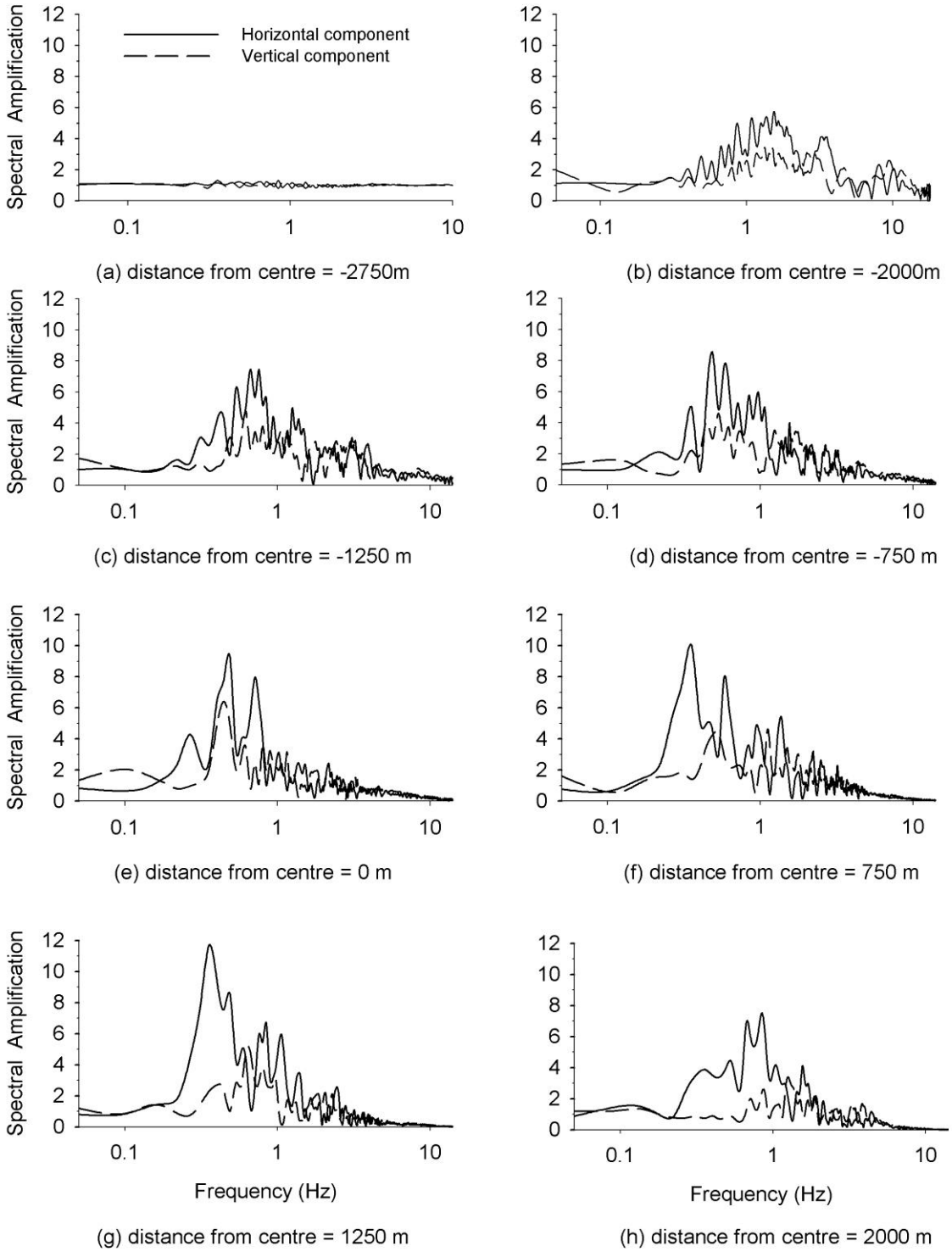

Figure 4.22 BTR waves spectral amplification for MS1 model.

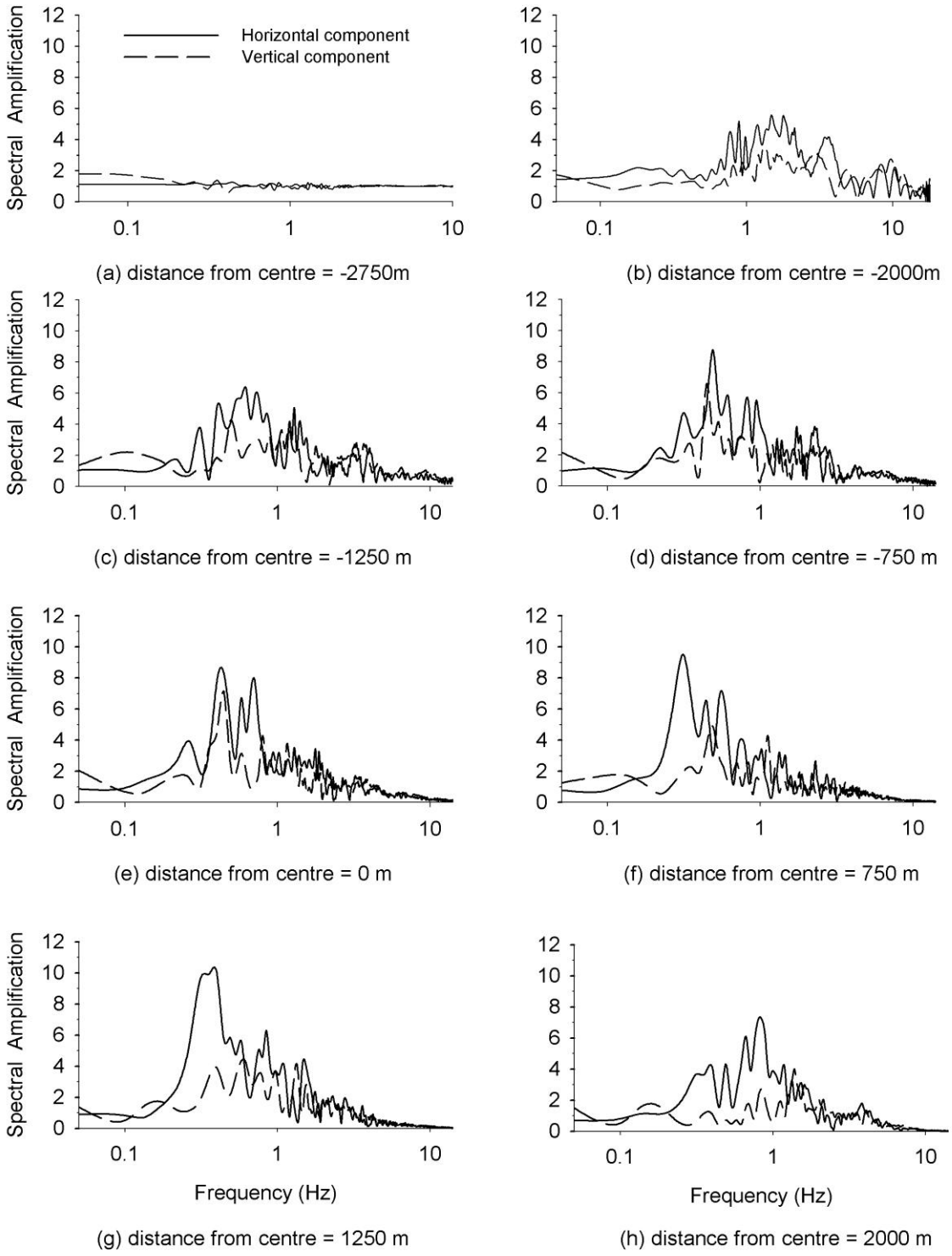

Figure 4.23 BTR waves spectral amplification for MS2 model.

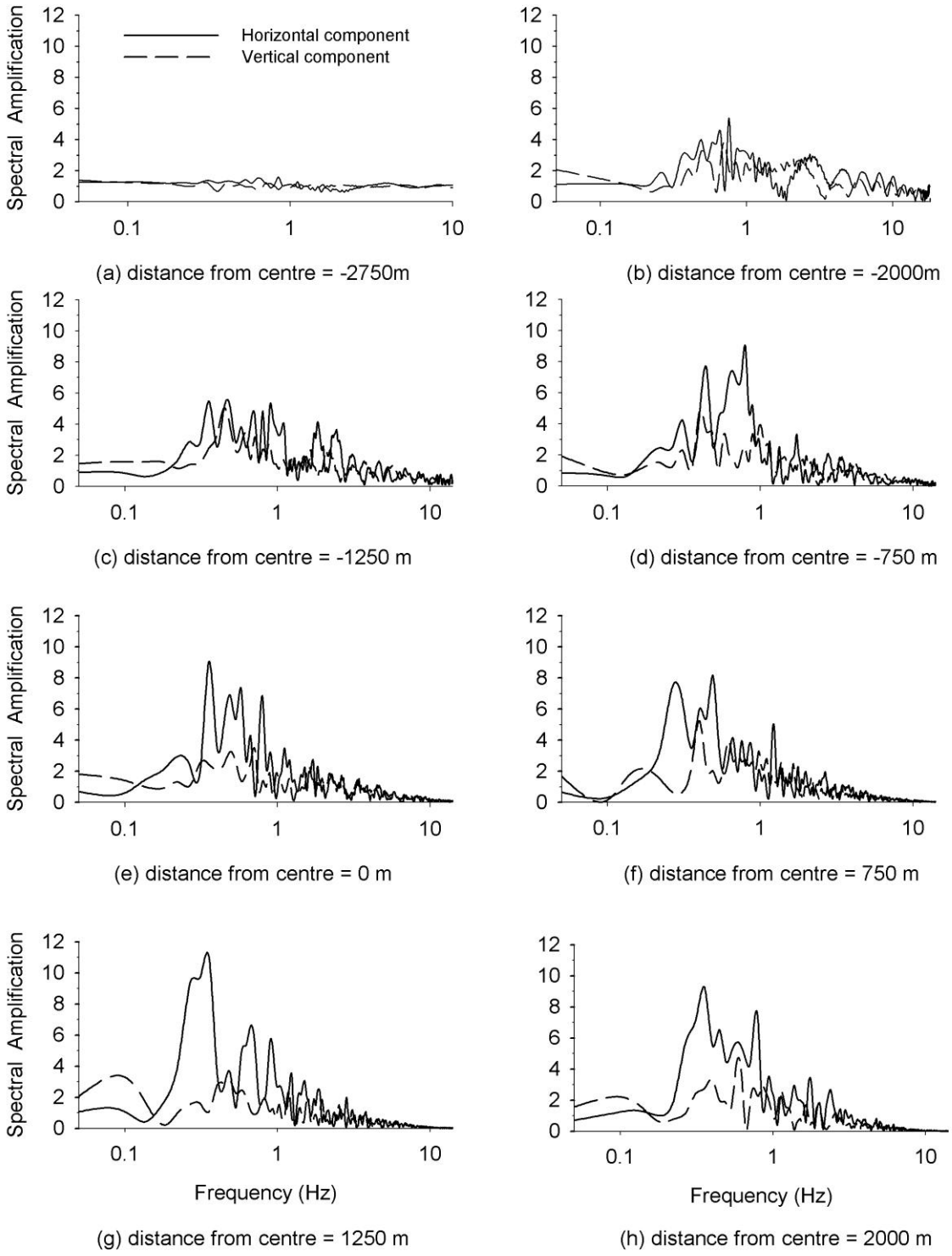

Figure 4.24 BTR waves spectral amplification for MS3 model.

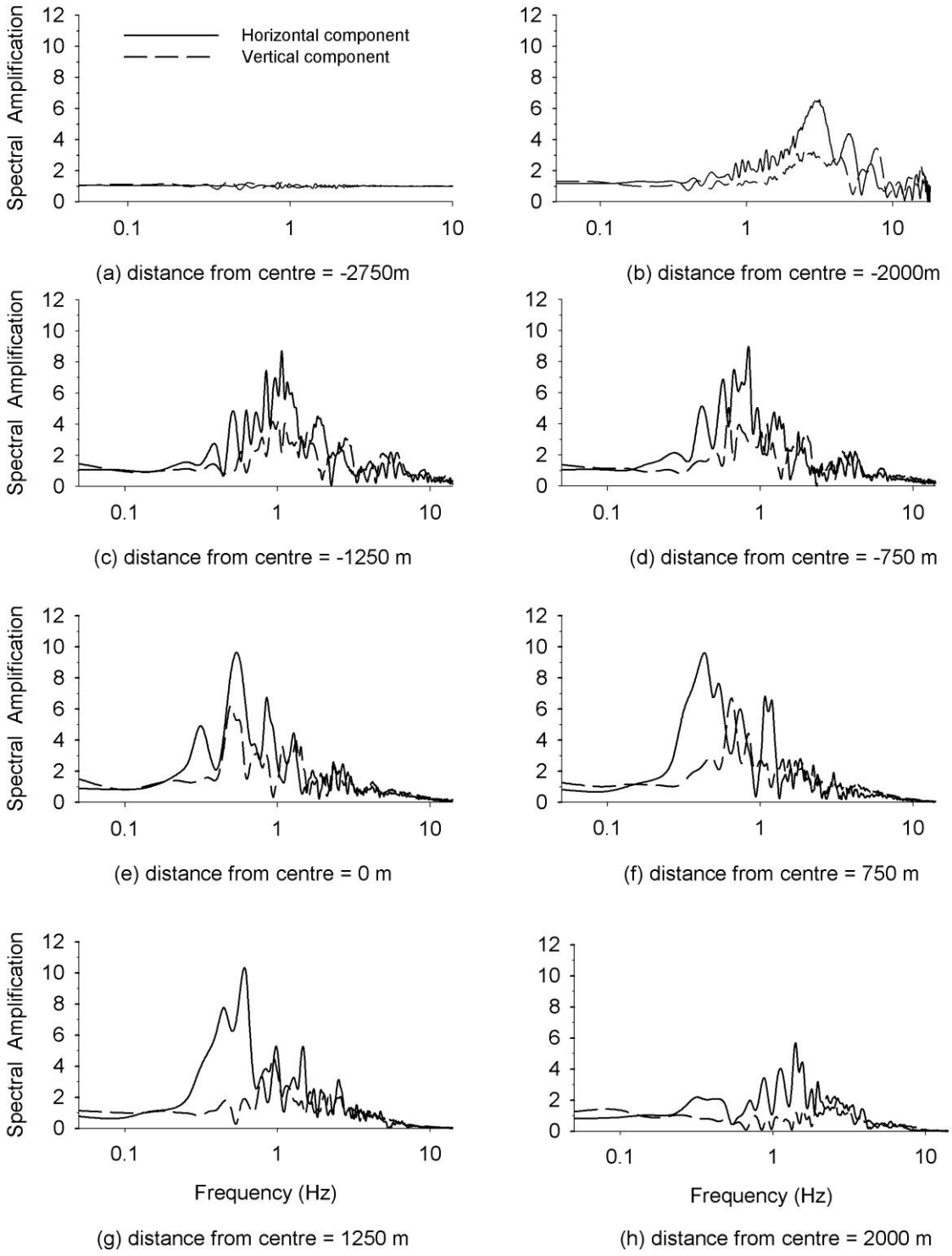

Figure 4.25 BTR waves spectral amplification for MS4 model.

The lowest ASA value was obtained corresponding to MS3 model which is trapezoidal model with steep slope in both the components. The ASA value for horizontal component was found higher than the vertical component. The largest value is obtained at a distance of 500 m from the left basin edge in all the cases. The largest value of order 1.7 was found for model MS1, MS2 and MS4 for vertical component. Finally, it may be concluded that the shape of basin play a major role in the amplification and complex mode transformation of the BTR-waves.

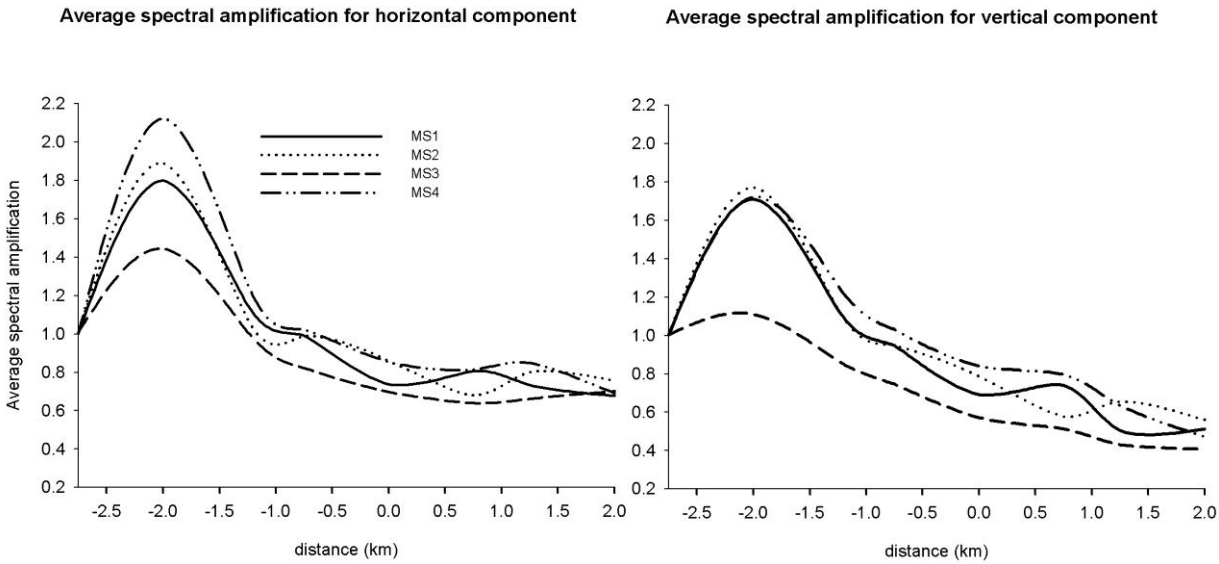

Figure 4.26 Average spectral amplification of BTR waves for different IC model (RIC1-RIC4)

CHAPTER # 5

STUDY OF EFFECTS OF IMPEDANCE CONTRAST ON THE BTR-WAVES

5.1 GENERAL:

To analyze the effects of impedance contrast (IC) on BTR waves at the basin edge, we have used different IC by varying the velocity of seismic waves and density in the rock. The velocity and other parameters of the basin was kept constant for different IC models. The basin model used in this case is elliptical with 600 m depth. Seismic response is computed at 25 stations out of which 21 stations are incorporated in the basin.

Table 5.1 shows the various parameters used in the RIC1-RIC4 rock models corresponding to the different IC models. Similarly, table 5.2 gives the different rheological parameters and the anelastic coefficients for RIC1-RIC4 rock models. The S-wave IC for the RIC1-RIC4 models are 3.5, 4.3, 4.9 and 6.0, respectively.

Table 5.1 Parameters for the RIC1-RIC4 models

MATERIAL/ IC MODELS	Vs (m/s)	Vp (m/s)	Density (g/cc)	Poisson ratio	Quality factor (Q_s)	Quality factor (Q_p)
RIC1	1750	3031	2.0	.25	175	303
RIC2	1800	3114	2.4	.25	180	180
RIC3	1900	3290	2.6	.25	190	329
RIC4	2000	3480	3.0	.25	200	348
Soil	500	971	2.0	.25	50	97

Table 5.2 Rheological parameters for different models of Impedance Contrast (RIC1 to RIC4 models).

Models	Unrelaxed moduli			Anelastic coefficients		
	μ_u (GPa)	**K** (GPa)	λ_u (GPa)	$Y_l^{\alpha}(1=1,4)$	Y_l^{β} (1=1,4)	$Y_l^{\lambda}(1=1,4)$
RIC1	5.92	17.64	5.78	0.00494	0.008355	0.009032139
				0.005119	0.008785	0.009516175
				0.003927	0.006736	0.007298516
				0.007393	0.012818	0.013909804
RIC2	7.86	23.42	7.69	0.005382384	0.009147663	0.009895534
				0.004554900	0.007794690	0.008440975
				0.004580726	0.007871273	0.008530337
				0.005516699	0.0095455956	0.010356537
RIC3	9.5	28.42	9.32	0.009089	0.007731	0.00836021
				0.00959	0.008105	0.008780876
				0.007352	0.006216	0.006735916
				0.014025	0.011803	0.012808562
RIC4	12.19	36.33	11.94	0.004348	0.007364	0.007963442
				0.00449	0.007707	0.008348853
				0.003445	0.005911	0.006404755
				0.006472	0.011211	0.01216399
SOIL	5.199	19.23	8.841	0.016374887	0.029520707	0.031454921
				0.014147617	0.026227224	0.028034256
				0.014406361	0.027163137	0.029101887
				0.017721045	0.034399170	0.036979010

Figures 5.1 to 5.4 show the horizontal and vertical components of the seismic responses of the RIC1 to RIC4 basin models. Analysis of these figures shows that the dispersion effect is almost similar in all the models responses since the velocity in the basin is kept same in all the cases. The later arrivals are more dispersed. It is also seen that earlier arrivals are very much affected by the velocity contrast between the rock and the basin.

Dispersion effects are seen more in case of RIC1 model. The amplitude of vertical component is higher than the horizontal component. A decrease of amplitude of BTR-waves in the basin is seen to be decreasing although there is an increase of IC (increase of the velocity in the rock). The increase of velocity and density in the rock is responsible for the decrease of amplitude of the SV-wave generated at the point source and finally the decrease of amplitude of the Rayleigh in the rock as well as in the basin.

5.2 Effect of IC on spectral amplification of BTR-wave

The spectral amplifications have been computed at 8 stations for both the components of the BTR-waves and is shown in figures 5.5-5.8. Out of considered 8 locations first one is at rock and rest are in basin. The analysis of these figures very clearly shows the increase of spectral amplification with the increase of IC, although it was not reflected in the time domain. Further, the increase of spectral amplification with IC is almost same for all the frequency for a particular IC. Overall, the amplification of the horizontal component is much more than that of the vertical component. The spectral amplification is of order 13 in the case of RIC4 model at a distance of 1250 m right of the basin.

Overall, amplification is larger in the lower frequency range, although there is minor shift in the frequency corresponding to larger amplification. In the lower frequency range, the amplification of the horizontal components is much more to that in the vertical components. It means lower frequency of the BTR-waves are horizontally polarized in the basin. Such highly amplified horizontally polarized BTR-waves may cause unexpected damage to the long-span structures.

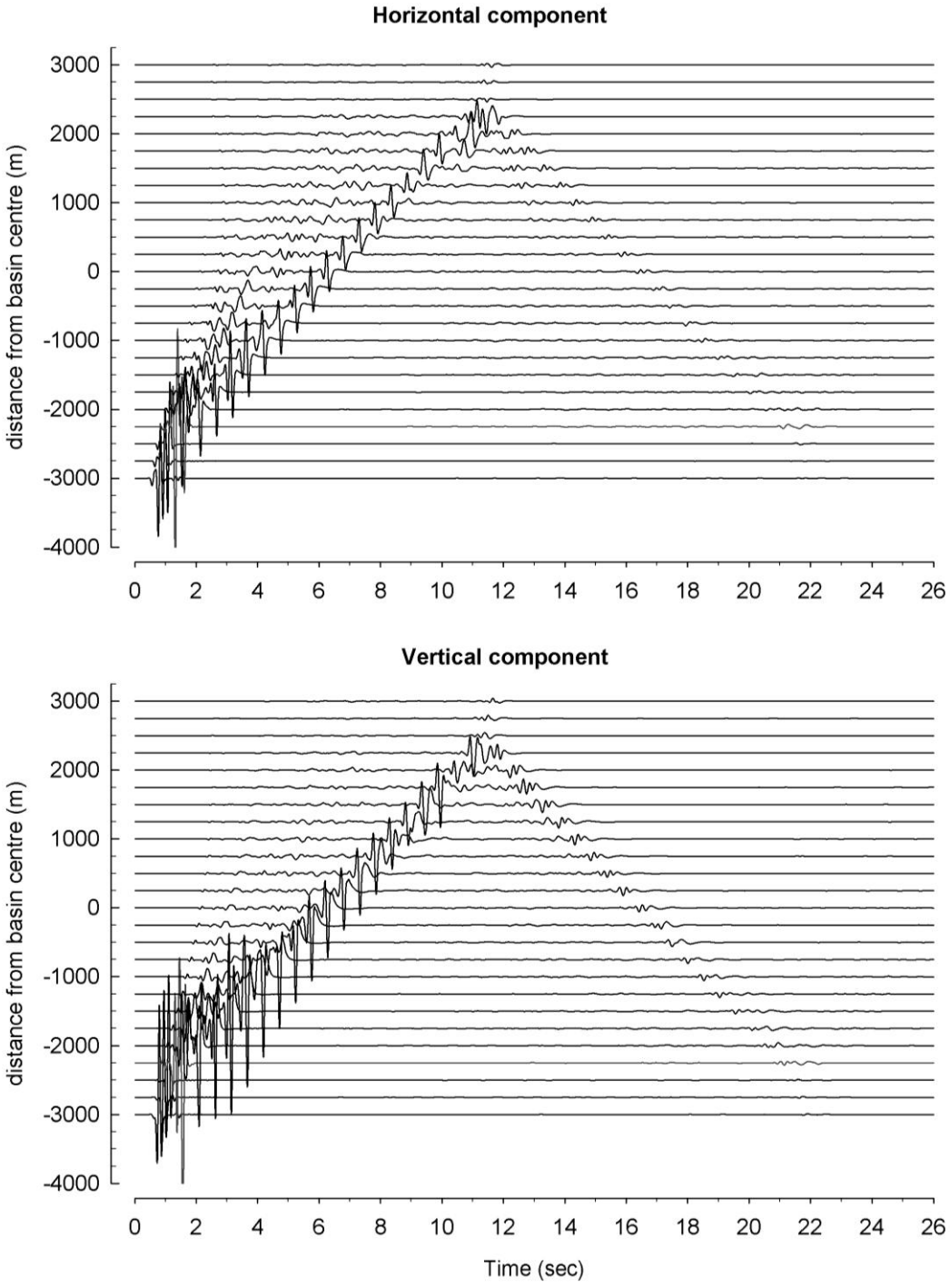

Figure 5.1 Seismic response of BTR waves at 25 stations for model RIC1

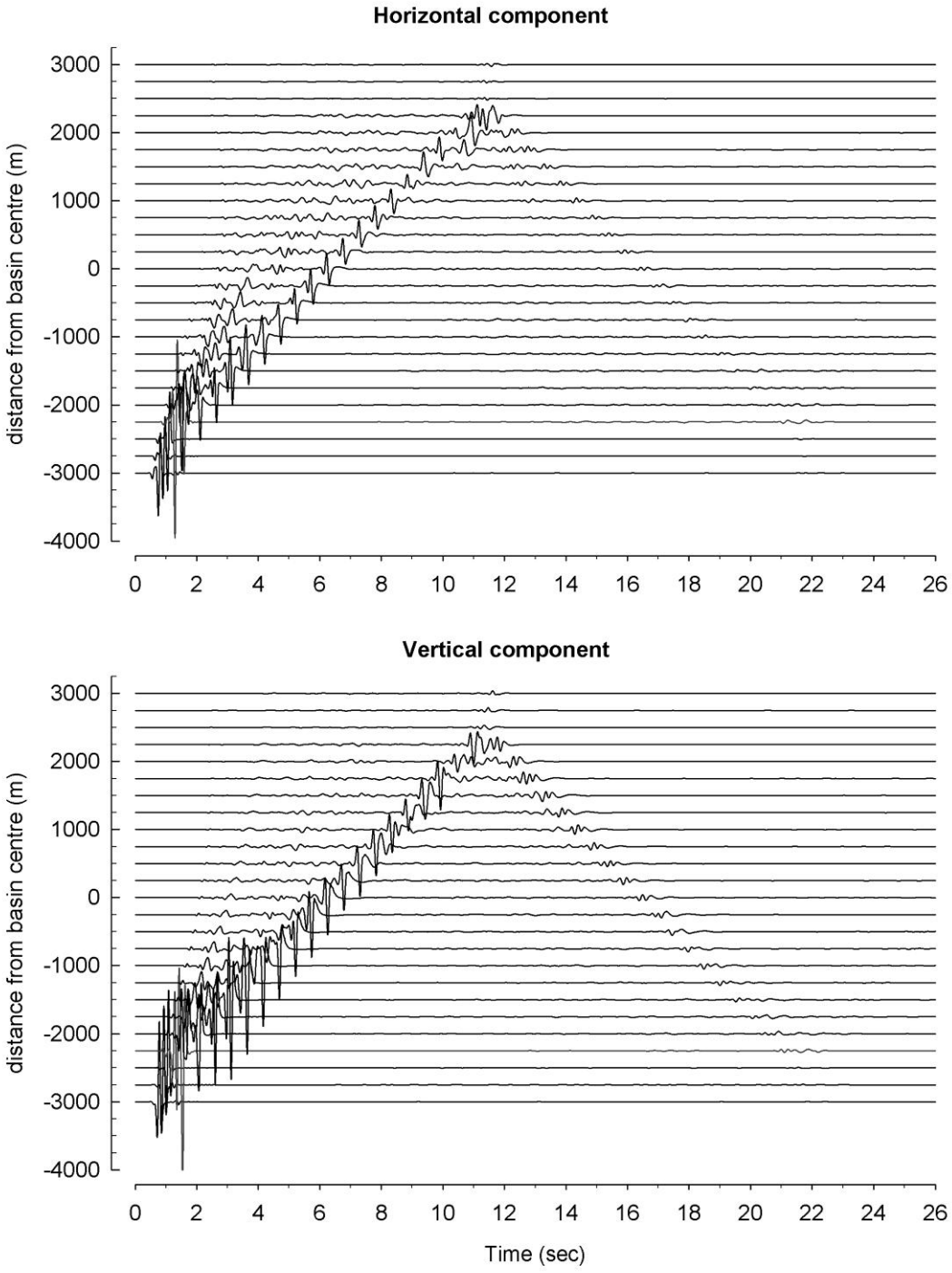

Figure 5.2 Seismic response of BTR waves at 25 stations for model RIC2

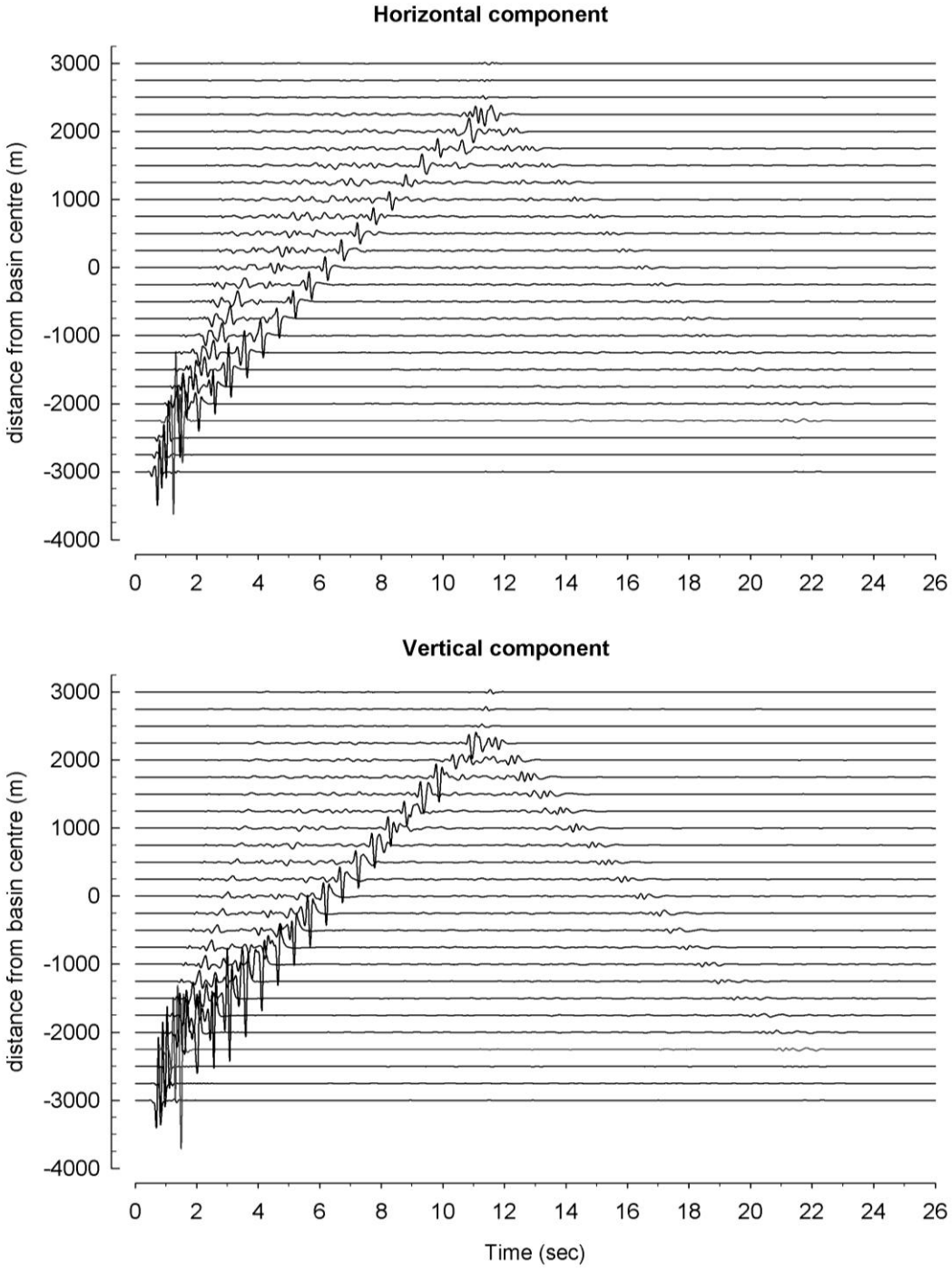

Figure 5.3 Seismic response of BTR waves at 25 stations for model RIC3

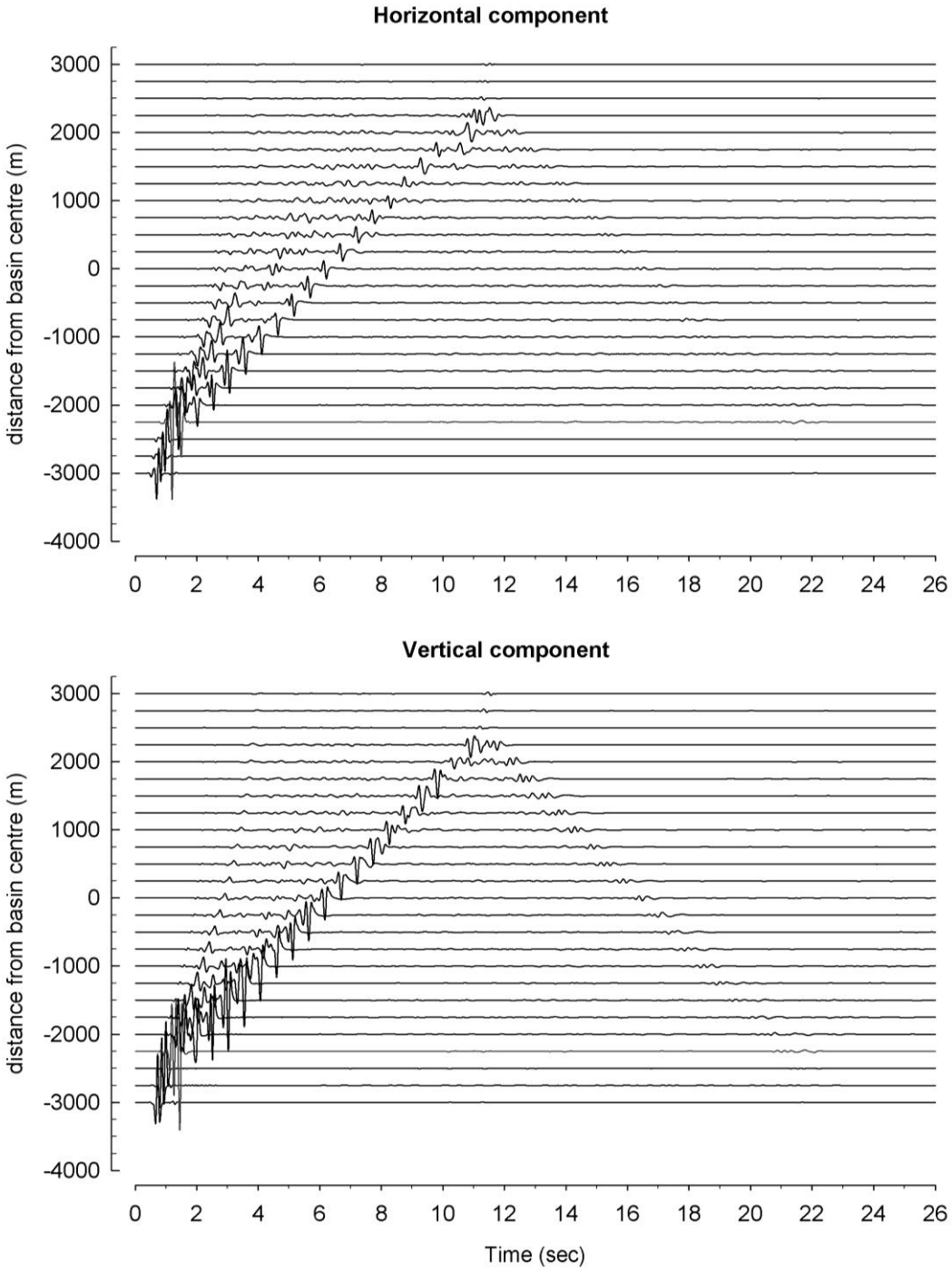

Figure 5.4 Seismic response of BTR waves at 25 stations for model RIC4

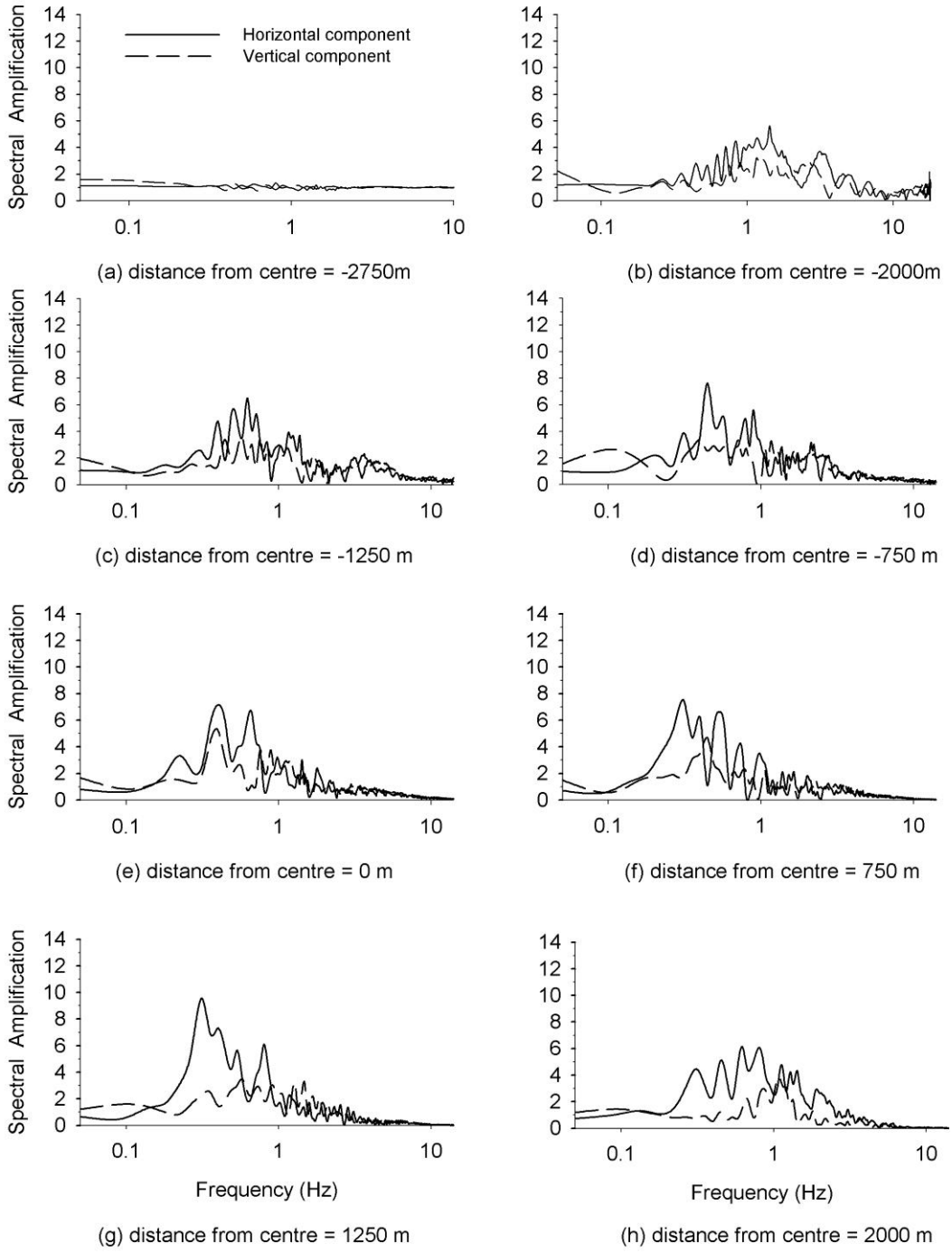

Figure 5.5 BTR waves spectral amplification for RIC1 model.

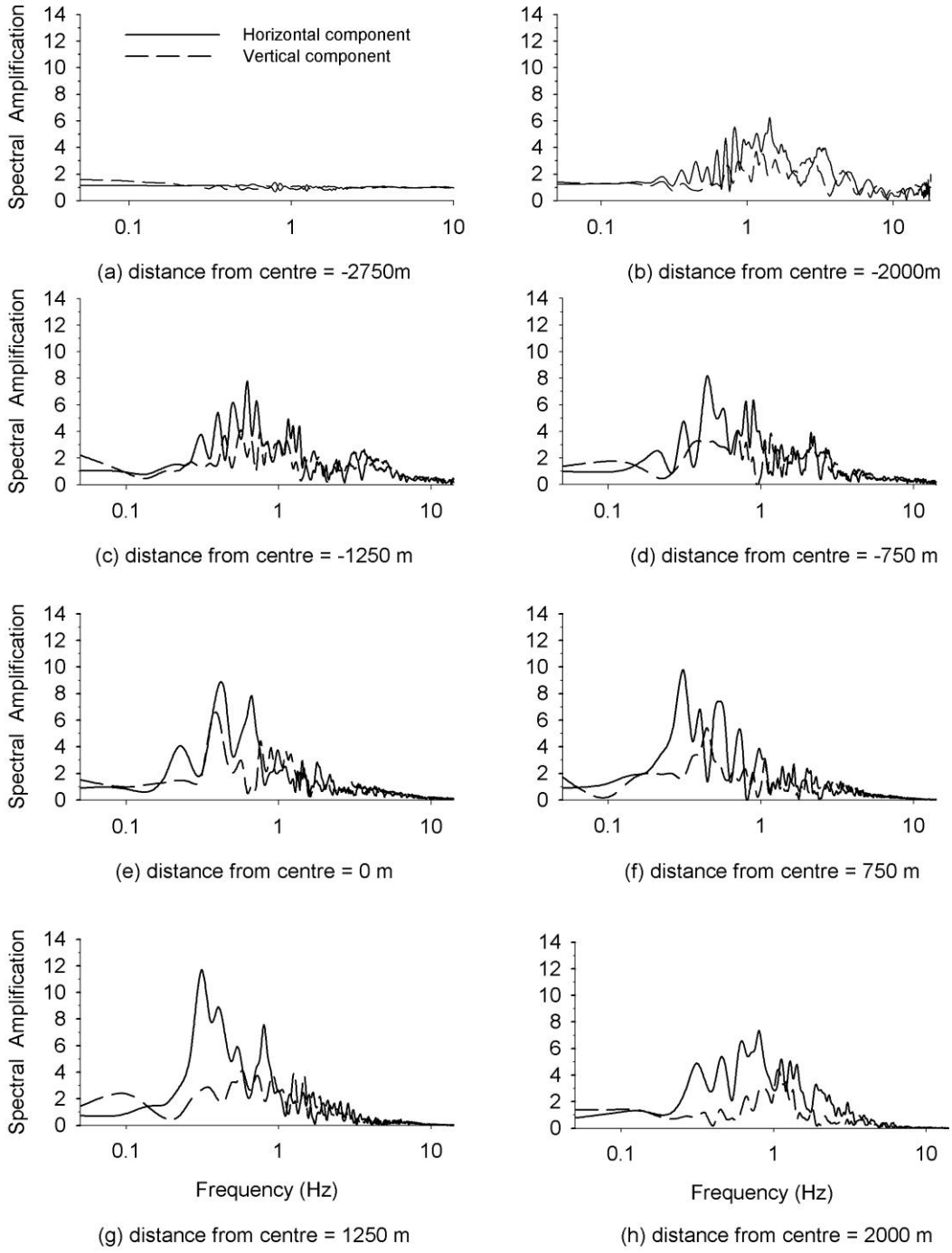

Figure 5.6 BTR waves spectral amplification for RIC2 model.

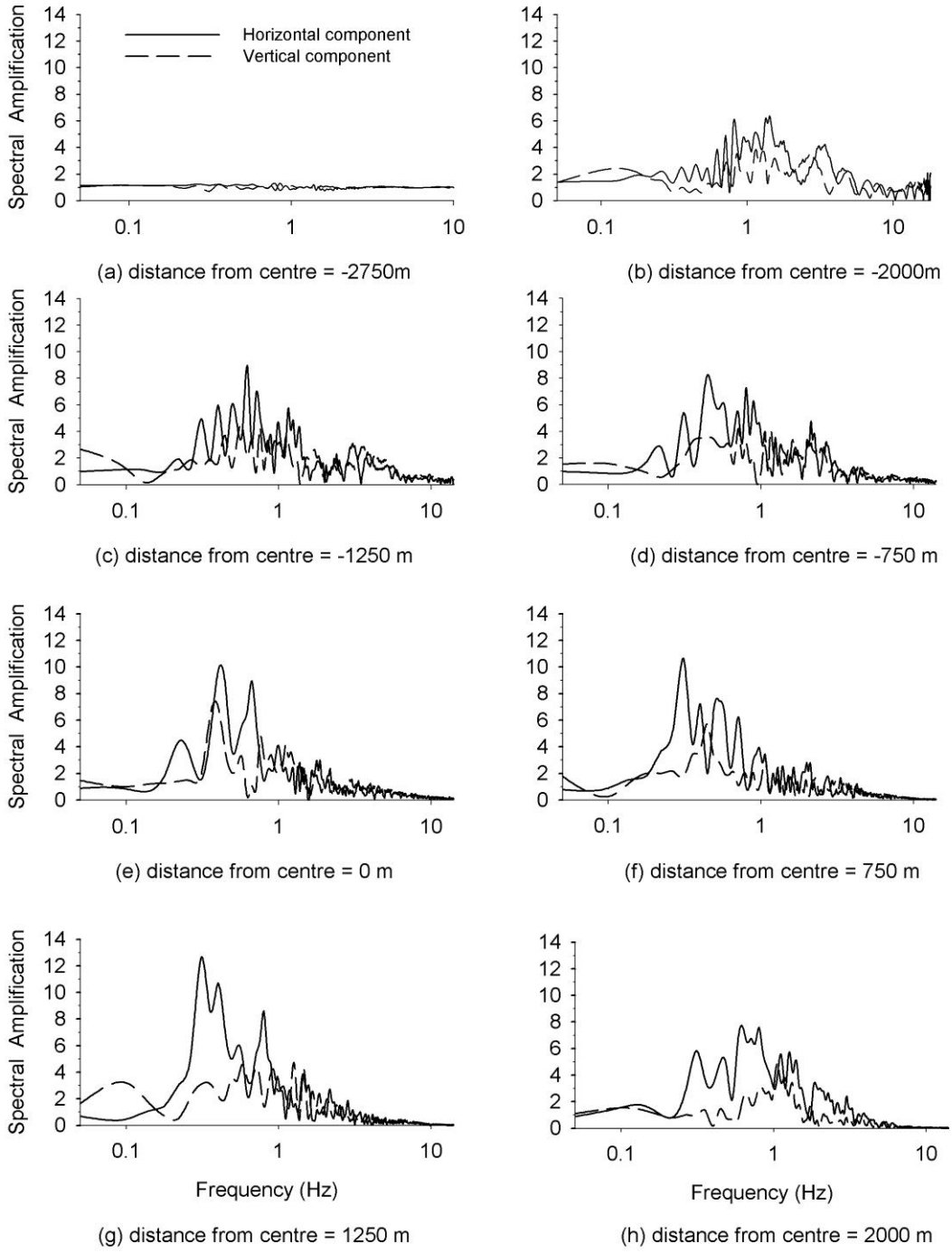

Figure 5.7 BTR waves Spectral amplification for RIC3 model.

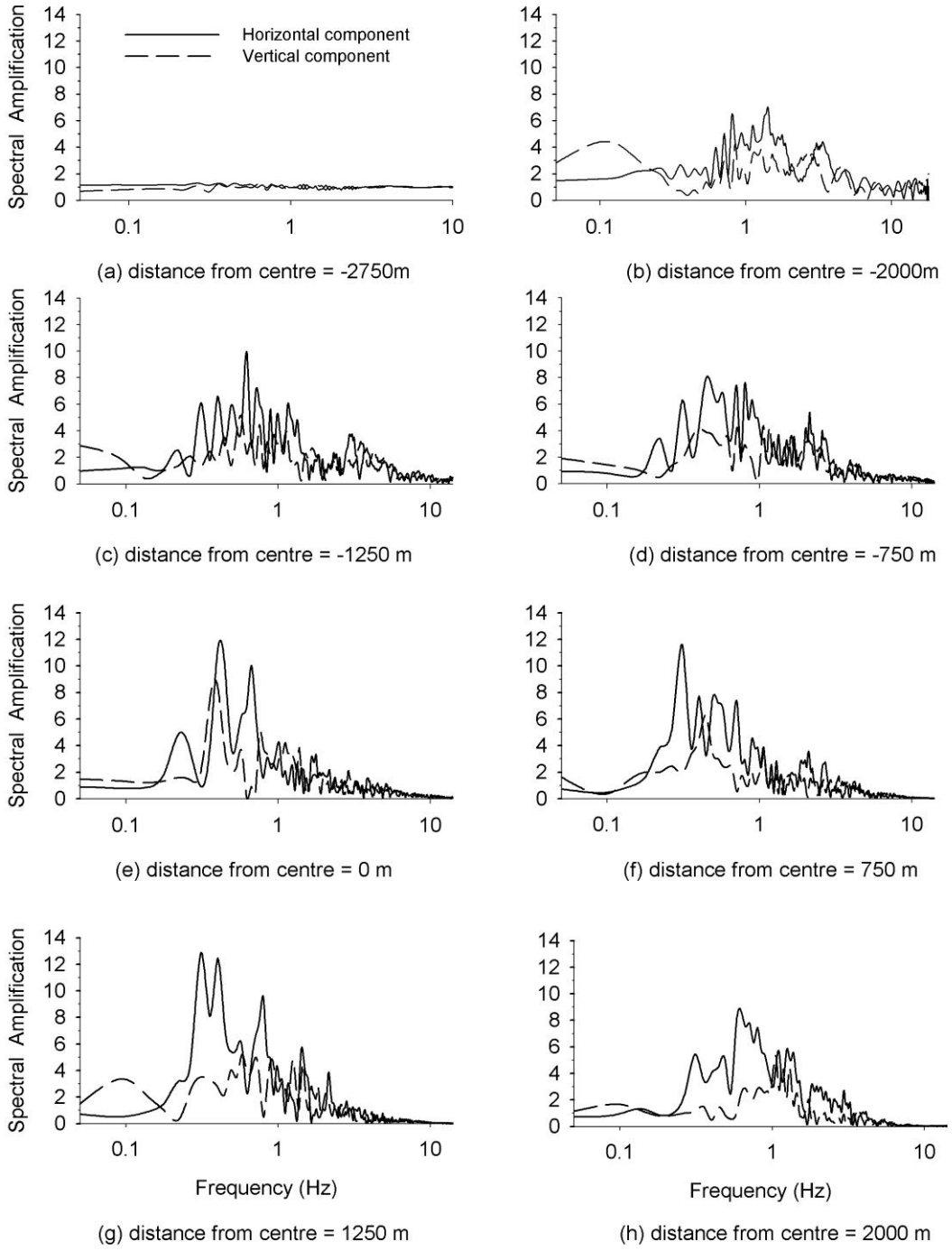

Figure 5.8 BTR waves Spectral amplification for RIC4 model.

5.3. Average spectral amplification of BTR wave

The average spectral amplification for the horizontal and the vertical components of the BTR waves were computed for different RIC1 to RIC4 models and is shown in figure 5.9. The analysis of the figure shows that highest value of average spectral amplification is obtained corresponding to RIC2 model at a distance of around 2.0 km towards the left of centre of basin in both the components. The least ASA is obtained in RIC1 model. Near the left edge of the basin, there is almost an increase of ASA with IC, except for RIC2 model in both the components. It reflects that IC also play a role in the mode transformation of the BTR-waves at the basin-edge. The largest average spectral amplification is of the order 2.1 for the horizontal component. The ASA value for horizontal component is higher than the vertical component in all the models. The value of ASA is increasing with IC at the centre of basin in the horizontal components and it is almost same in the vertical components except RIC1model. There is an increase of ASA towards the right edge of the basin due to the reflected BTR-waves from the right-edge of the basin.

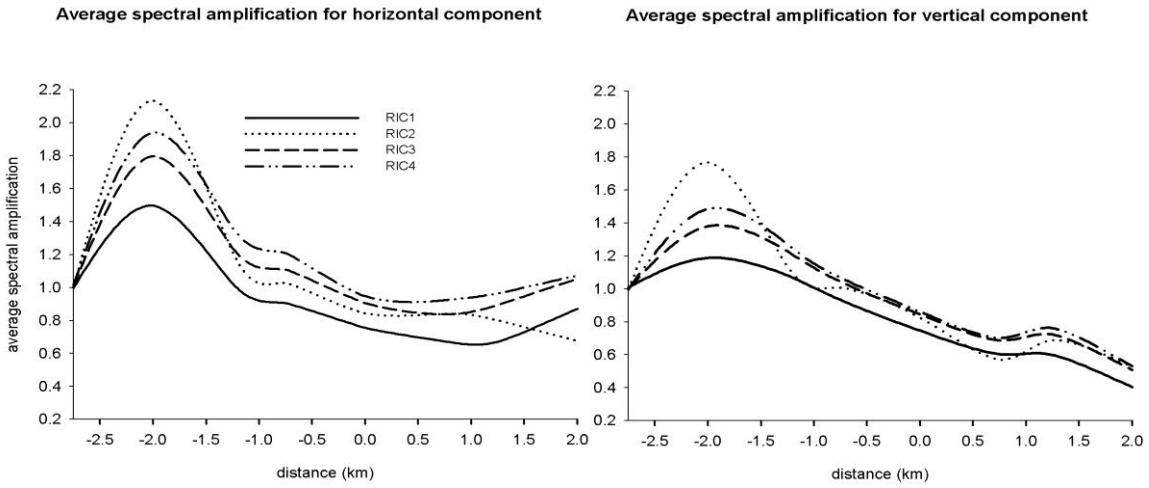

Figure 5.9 Average spectral amplification of BTR waves for different IC model (RIC1-RIC4)

CHAPTER # 6

CONCLUSIONS

A fourth order staggered grid viscoelastic P-SV wave FD program was used for the simulation of Rayleigh wave responses of the basin models (Narayan and Kumar, 2014). The Gabor wavelet was used as a source excitation function. The simulation was also carried out for homogeneous model. The simulated of Rayleigh wave response of the homogeneous half-space model showed that the Rayleigh waves are vertically polarised. The interaction of the Rayleigh wave with the basin edge caused the complex mode transformation and amplification of the BTR waves at the edges. Different modes of Rayleigh waves having both horizontally and vertically polarized one were observed in the basin. The study showed lesser dispersion of the horizontally polarized Rayleigh wave. The interaction of Rayleigh waves with the basin edges has developed both the body as well as the surface waves in the basin. From the analysis of the various models it was concluded that the spectral amplification of the BTR waves depend on the basin depth, shape and impedance contrast at the edge of the basin.

The amplitude of the horizontally polarised fast moving BTR-wave is decreasing with an increase of depth of basin. In contrast to this, the amplitude of the vertically polarised slow moving BTR-wave is increasing with an increase of depth of basin. Further, an increase of reflection of the BTR-waves with an increase of depth of basin can be inferred. The shape of spectral amplification is varying largely from the basin edge as the depth increases.The amplification is larger in the case of lesser soil thickness near the basin edge. The spectral amplification is of order 9 times in case of 400 m depth basin at very low frequency. At higher frequency the spectral amplification decreases as the depth increases in case of horizontal component. Towards the end of the basin the largest amplification is obtained corresponding to the 600 m depth basin which may be due to the effects of edge reflections. The highest amplification of the horizontal component of Rayleigh waves of order 11

was obtained corresponding to 300 m depth. The ASA value of horizontal component was higher than the vertical component when the basin depth was less than 400 m, afterwards both the components are become nearly same. The largest ASA value was found corresponding to 100 m depth.

Analysis of simulated response corresponding to the different basin shape showed that the largest value of spectral amplitude increases as the slope of the basin edge increases. The simulated response of elliptical model was found to be similar to the trapezoidal model with gentle slope. In case of very large wavelength of Rayleigh waves (frequency less than 0.1 Hz), there was no amplification of both the components of the BTR-waves. The triangular model showed highest spectral amplification of order 2.2 in the horizontal component. The lowest ASA value was obtained corresponding to MS3 model which is trapezoidal model with steep slope in both the components. The ASA value for horizontal component was found higher than the vertical component. The largest value of ASA is obtained near the basin edge in all the cases. The largest value of order 1.7 was found in the vertical component. Finally, it may be concluded that the shape of basin play a major role in the amplification and complex mode transformation of the BTR-waves.

The analysis of different IC model showed the increase of spectral amplifications with the increase of IC. The spectral amplification is of order 13 in the case of the highest IC model (6.0) towards the end of the basin. There is almost an increase of ASA with IC, except for RIC2 model in both the components. There is an increase of ASA towards the right edge of the basin due to the reflected BTR-waves from the right-edge of the basin.

REFERENCES

1. Clayton, R.W., and Engquist, B. (1977), Absorbing boundary conditions for acoustic and elastic wave equations, Bull. Seism. Soc. Am., 67, 1529–1540.
2. Emmerich, H. and M. Korn,(1987). Incorporation of attenuation into time-domain computations of seismic wave fields. Geophysics 52, 1252-1264
3. HANKS, T. C. (1975) Strong Ground Motion of the San Fernando, California Earthquake: Ground Displacements, Bull. Seism. Soc. Am., 65, 193-225
4. Futterman, W. I., (1962). Dispersive body waves. Journal of Geophysics Research 67, 5279 -5291
5. Israeli, M., and S.A. Orszag (1981), Approximation of radiation boundary conditions, J. Comp. Phys. 41, 115-135, DOI: 10.1016/0021-9991(81)90082-6.
6. Kawase, H., (2002). Site effects on strong ground motions in 'International Handbook of Earthquake andEngineering Seismology, Ed. Lee et al.', part B, chapter 61, 1013-1030.
7. Kawase, H., (1993). Effects of surface and subsurface irregularities in Earthquake and ground motions',Architectural Institute of Japan, part 1, chapter 3, 118-155.
8. Kristek, J., Moczo, P., (2003). Seismic wave propagation in viscoelastic media with material discontinuities– a 3D 4th-order staggered-grid finite-difference modeling. Bulletin of the Seismological Society of America, 93, 2273-2280.
9. Kumar, S., and J.P. Narayan (2008), Absorbing boundary conditions in a fourthorderaccurate SH-wave staggered grid finite difference algorithm, ActaGeophysica, 56, 4, 1090-1108
10. KRAMER, S.L. (2004) Geotechnical Earthquake Engineering, Second Indian reprint, Pearson Education.
11. Levander, A.R., (1988). Fourth-order finite-difference P-SV seismograms. Geophysics 53, 1425-1436.
12. Narayan, J.P. and Kumar, S., (2010). Study of effects of focal depth on the characteristics of Rayleigh waves using finite-difference method. Acta Geophysica 58, 624-644.

13. Narayan, J.P., (2010). Effects of impedance contrast and soil thickness on the BTR waves and associated differential ground motion. Pure and Applied Geophysics 167, 1485-1510.
14. Narayan, J.P., (2012). Effects of P-wave and S-wave impedance contrast on the characteristics of BTR waves. Pure and Applied Geophysics DOI 10.1007/s00024-011-0338-7.
15. Pitarka, A. (1999), 3-D elastic finite difference modelling of seismic motion usingstaggered grids with variable spacing, Bull. Seism. Soc. Am. 89, 54-68.
16. Virieux, J. (1986), P-SV wave propagation in heterogeneous media, velocity stress finite-difference method, Geophysics 51, 889-901, DOI: 10.1190/1.1442147.